



UNIVERSIDADE ESTADUAL DE CAMPINAS
INSTITUTO DE BIOLOGIA

VIVIANE LUCIA BERALDO DE ARAÚJO

CARREADORES LIPÍDICOS NANOESTRUTURADOS (NLC)
COM LIDOCAÍNA: SCREENING POR DELINEAMENTO DE
HALL

NANOSTRUCTURED LIPID CARRIERS (NLC) CONTAINING
LIDOCAINE: SCREENING BY HALL DESIGN

CAMPINAS

2018

VIVIANE LUCIA BERALDO DE ARAÚJO

**CARREADORES LIPÍDICOS NANOESTRUTURADOS (NLC) COM
LIDOCAÍNA: SCREENING POR DELINEAMENTO DE HALL**

**NANOSTRUCTURED LIPID CARRIERS (NLC) CONTAINING
LIDOCAINE: SCREENING BY HALL DESIGN**

Dissertação apresentada ao Instituto de Biologia da Universidade Estadual de Campinas como parte dos requisitos exigidos para a obtenção do Título de Mestra em Ciências, na área de concentração em Fármacos, Medicamentos e Insumos para Saúde.

Dissertation presented to the Institute of Biology of the University of Campinas in partial fulfillment of the requirements for the degree of Master in Sciences, in the field of Drugs, Medicines and Health Supplies.

ESTE ARQUIVO DIGITAL CORRESPONDE À VERSÃO FINAL DA DISSERTAÇÃO DEFENDIDA PELA ALUNA VIVIANE LUCIA BERALDO DE ARAÚJO E ORIENTADA PELA PROFa. Dra. LAURA DE OLIVEIRA NASCIMENTO.

Orientador: LAURA DE OLIVEIRA NASCIMENTO

CAMPINAS

2018

Agência(s) de fomento e nº(s) de processo(s): CAPES
ORCID: <https://orcid.org/0000-0002-6868-5208>

Ficha catalográfica
Universidade Estadual de Campinas
Biblioteca do Instituto de Biologia
Mara Janaina de Oliveira - CRB 8/6972

B45c Beraldo-de-Araujo, Viviane Lucia, 1983-
Carreadores lipídicos nanoestruturados (NLC) com lidocaína: screening por delineamento de Hall / Viviane Lucia Beraldo de Araújo. – Campinas, SP : [s.n.], 2018.

Orientador: Laura de Oliveira Nascimento.
Dissertação (mestrado) – Universidade Estadual de Campinas, Instituto de Biologia.

1. Carreadores lipídicos nanoestruturados. 2. Excipientes. 3. Lipídeos. 4. Análise multinível. 5. Liberação controlada de fármacos. I. Nascimento, Laura de Oliveira, 1980-. II. Universidade Estadual de Campinas. Instituto de Biologia. III. Título.

Informações para Biblioteca Digital

Título em outro idioma: Nanostructured lipid carriers (NLC) containing lidocaine: screening by Hall design

Palavras-chave em inglês:

Nanostructured lipid carriers

Excipients

Lipids

Multilevel analysis

Controlled drug delivery

Área de concentração: Fármacos, Medicamentos e Insumos para Saúde

Titulação: Mestra em Ciências

Banca examinadora:

Laura de Oliveira Nascimento [Orientador]

Francisco Benedito Teixeira Pessine

Karina Cogo Müller

Data de defesa: 06-02-2018

Programa de Pós-Graduação: Biociências e Tecnologia de Produtos Bioativos

Campinas, 06 de fevereiro de 2018.

COMISSÃO EXAMINADORA

Profa. Dra. Laura de Oliveira Nascimento

Prof. Dr. Francisco Benedito Teixeira Pessine

Profa. Dra. Karina Cogo Müller

Os membros da Comissão Examinadora acima assinaram a Ata de Defesa, que se encontra no processo de vida acadêmica do aluno.

EPÍGAFRE

*Podemos facilmente perdoar uma criança que tem medo do escuro;
a real tragédia da vida é quando os homens têm medo da luz.*

Platão, A República

AGRADECIMENTOS

Agradeço a Deus, pela honra e privilégio de chegar onde cheguei, depois de tanta batalha, estudando em escolas públicas, me qualificar em uma das melhores universidades da América Latina e fazer o que gosto: estudar, “mexer nos vidrinhos” e nunca parar de aprender.

Agradeço à minha orientadora, Laura de Oliveira Nascimento, por ter acreditado em mim desde o início, por se sentir parte e, muitas vezes, mostrar a mim mesma as qualidades do meu trabalho, sabendo lidar com minha teimosia. Pelo apoio incondicional e fraterno quando soube que sua aluna seria mãe, e por me auxiliar em todo o processo de afastamento e retorno às atividades acadêmicas, tornando-os menos árduos.

Agradeço também às valiosas sugestões e contribuições feitas pelos membros da minha banca de qualificação, professores Paulo Rosa, Cíntia Cereda e Francisco B. T. Pessine, por quem tenho muito carinho e admiração desde minha época de Iniciação Científica em seu laboratório.

Agradeço à FAPESP (n° 14/14457-5) e CAPES pelo apoio financeiro. Ao Instituto de Biologia por propiciar a estrutura sobre a qual pude conduzir meu trabalho, em especial ao Laboratório de Biomembranas, conduzido pela professora Eneida de Paula. À Faculdade de Ciências Farmacêuticas, que me abrigou ao final do meu projeto. Em especial, ao secretário do Programa de Pós-Graduação de Biociências e Tecnologia de Produtos Bioativos, Rafael Pessoa, por ter sido sempre solícito e me atendido nas mais diversas dúvidas.

Agradeço aos meus colegas do Latef: Juliana Costa, pela amizade, conselhos e toda a colaboração. Danilo Geraldes, pela generosidade e ser um bom guia gastronômico. Ana Pelegrine e Ingrid Vaz, minhas queridas alunas de iniciação científica que tanto me ajudaram na condução do meu trabalho.

Agradeço às “Pessinetes”: Letícia, Ana Cláudia, Milene, Daniela, Luciana, pelas quais tenho muito carinho e admiração. Obrigada, em especial, à Letícia, pelas valiosas contribuições teóricas e práticas.

Agradeço a todos que, de alguma forma, me auxiliaram durante essa jornada: Verônica Couto, Glazieli Marangoni, Viviane Guilherme, Simone Castro, Lígia Nunes.

Agradeço à Gleisy Picoli, pela amizade que o curso de Filosofia me rendeu. Pelos conselhos, cafés, cervejas, por ser o ombro amigo e por transformar qualquer assunto em algo risível. E viva Dioniso!

À minha família: agradeço aos meus pais, Lúcia e Vadiney, por terem me proporcionado a base emocional e racional, sobre a qual eu pude me apoiar para buscar meus objetivos. Aos meus irmãos, Erick e Patrícia, por fazerem parte de quem eu sou. Ao meu sobrinho, Enzo, pela alegria contagiatante e por nos tirar um sorriso quando menos esperamos.

À “vovó postiça” Valéria, que me ajudou a cuidar do Antoni nos momentos mais difíceis como se fosse seu próprio neto.

Por último, mas não menos importantes, agradeço ao meu marido, Anderson, pelo companheirismo, colaboração estatística e por acreditar mais em mim do que eu mesma. Você me faz manifestar o melhor de mim. E ao homenzinho da minha vida, Antoni, que nasceu no meio do meu mestrado, e me faz aprender a cada dia a importância do amor e doação ao próximo.

RESUMO

Para formular racionalmente nanopartículas, é fundamental conhecer as interações entre seus excipientes e como eles podem alterar as características físico-químicas das nanopartículas. Essa é uma questão crítica principalmente no *screening* e desenvolvimento de carreadores lipídicos nanoestruturados (NLCs) porque eles são produzidos com pelo menos três tipos de excipientes (lipídio sólido, óleo e tensoativo). Exaustivas combinações de excipientes e comparações para determinar suas influências no delineamento de NLCs tem sido desenvolvidas, mas sem uma perspectiva prática para quantificar a interação sinergística entre os seus componentes. Propomos nesse trabalho uma abordagem inovadora para analisar o efeito das interações dos excipientes nas propriedades físico-químicas das NLCs, o que pode ter um grande impacto na forma como os pesquisadores desenvolvem nanocarreadores. Ademais, nossa metodologia permite analisar o efeito de até 15 excipientes com poucas formulações. Isso proporciona um caminho prático para fazer *screening* de excipientes e permite o desenvolvimento de nanocarreadores com as características desejadas previamente estabelecidas. O método consiste de dois experimentos sequenciais empregando delineamento de Hall, modelagem matemática com modelos mistos e análise multiníveis. As NLCs foram produzidas pelo método de emulsificação-ultrasonicação à quente. Os parâmetros de entrada para a análise das NLCs foram: lidocaína, como modelo de fármaco hidrofóbico, e nove excipientes; os parâmetros de saída foram z-average (tamanho médio, medido por Espalhamento Dinâmico de Luz, DLS), índice de polidispersidade (PDI, medido por DLS), potencial zeta (DLS), eficiência de encapsulação (HPLC) e capacidade de carga (HPLC). Todos os modelos de regressão linear para os experimentos exibiram valor de efeito considerável, com significativa estatística – F ($p = 0,01$). Para todos os parâmetros de saída, o segundo experimento permitiu melhor ajuste que o primeiro, com significativo valor F ($p = 0,02$), o que permitiu avaliar as interações com base nos modelos do segundo experimento. A partir disso, óleo de rícino (CA), palmitato de cetila (CP), ácido cáprico/caprílico (CC) e polisorbato 80 (PS) foram os excipientes que apresentaram os maiores efeitos, assim como um padrão de interações sinergísticas entre eles. Para confirmar alguns dos resultados obtidos, uma NLC feita com cera de abelha (BW), CA, PD e lidocaína foi analisada e exibiu o padrão predito nos modelos quanto às características físico-químicas. Esse resultado mostra a robustez do método desenvolvido, podendo ser aplicado não apenas para NLCs, mas também para a produção de outros tipos de nanopartículas.

Palavras-chave: Carreadores lipídicos nanoestruturados, lipídios naturais, análise multinível, delineamento de Hall, lidocaína

ABSTRACT

To rationally formulate nanoparticles, it is crucial to know the interaction among their excipients and how they change physicochemical attributes of nanoparticles. This is especially critical for the screening and development of nanostructured lipid carriers (NLCs) because they are made of at least three types of excipient (solid lipid, oil and surfactant). Exhaustive combinations of excipients and comparisons to assess their influence on the design of NLCs have been performed, but with no practical perspective to quantify synergistic interaction of NLCs components. In this work, we propose an innovative approach to analyze the effect of excipient interactions on physicochemical properties of NLCs, which can have a great impact on the way the researches develop nanocarriers. Indeed, our method permits to analyze the effects of many excipients (up to 15) with few formulations. This provides a practical pathway to make screening of excipients and allows to develop nanocarriers with the desirable predicted characteristics. It compasses two sequential experiments with Hall design, mathematical modelling with mixed models and multilevel statistics. NLCs were prepared by hot emulsification-ultrasonication method. The inputs of NLCs analysis were lidocaine as the hydrophobic model drug and nine excipients; the outputs were z-average (size, measured by Dynamic Light Scattering, DLS), polydispersity index (PDI, measured by DLS), zeta potential (DLS), entrapment efficiency (HPLC) and drug loading of NLCs (HPLC). All the linear regression models for the experiments exhibited good effect values with significant F-statistics ($p = 0.01$). For all outputs, the second experiment permitted higher fitting than the first one, with significant F-statistics ($p = 0.02$). This allowed evaluating the interactions based on the models of the second experiment. Hence, castor oil (CA), cetyl palmitate (CP), capric/caprylic acid (CC) and polysorbate 80 (PS) presented larger effects among the excipients as well as a clear pattern of synergistic interactions among them. To confirm some of the outcomes, a NLC made of beeswax (BW), CA, PS and lidocaine was analyzed and exhibited the predicted pattern of the physicochemical characteristics. This shows the robustness of the methodology, which can be applied not only to NLCs but also to the production of other nanoparticles.

Keywords: Nanostructured lipid carriers, natural lipids, multilevel analysis, Hall design, lidocaine

Lista de ABREVIATURAS E SIGLAS

%EE	Eficiência de Encapsulação / Entrapment Efficiency
AL	Anestésico Local
CA	Cera de Abelha
CCD	Charge Coupled Device - Dispositivo de Carga Acoplado
CLD	Conjugado Lipídio-Fármaco
CLS	Classical Least Squares
CP	Palmitato de Cetila
DDS	Drug Delivery Systems - Sistemas de Entrega de Fármacos
	Differential scanning calorimetry - Calorimetria Diferencial de
DSC	Varredura
	High Performance Liquid Chromatography - Cromatografia Líquida
HPLC	de Alta Eficiência
KOL	Kolliphor® (Poloxamer 188)
LD	Lidocaína
LL	Lipídio líquido
LS	Lipídio sólido
MET	Microscopia Eletrônica de Transmissão
MIGLYOL	Ácido cáprico/caprílico
	Nanostructured Lipid Carrier - Carreadores Lipídicos
NLC	Nanoestruturados
OG	Óleo de Gergelim
OR	Óleo de Rícino
PDI	Índice de Polidispersidade
SLN	Solid Lipid Nanoparticles - Nanopartículas Lipídicas Sólidas
V/V	Volume/Volume
ZP	Potencial Zeta / Zeta Potential
CP	Cetyl Palmitate
BW	Beeswax
SO	Sesame Oil
CO	Corn Oil
CS	Cottonseed Oil

CA Castor Oil
CC Capric/caprylic oil
PS Polysorbate 80
KO Poloxamer 188
LD Lidocaine
Exp 1 Experiment 1
Exp 2 Experiment 2

SUMÁRIO

1.	Introdução.....	14
2.	Objetivos.....	21
2.1.	Objetivo Geral	21
2.2.	Objetivos Específicos.....	21
3.	Capítulo I.....	22
1	introduction:	24
2	Methods:.....	27
2.1	Material	27
2.2	Lipids selection	27
2.3	Lidocaine solubility	27
2.4	Partition coefficient of lidocaine.....	28
2.5	Preparation of Nanostructured Lipid Carriers (NLC).....	28
2.6	LD Quantification, entrapment efficiency and drug loading:	28
2.7	Determination of hydrodynamic diameter (z-average), polydispersity index (PDI) and zeta potential (ζ)	29
2.8	Differential Scanning Calorimetry (DSC).....	29
2.9	LD in vitro release profile	29
2.10	Transmission electron microscopy.....	30
2.11	Design of Experiment (DoE) and statistical analysis.....	30
3	Results and discussion:	31
3.1	LD solubility and partition coefficient:	31
3.2	Thermal analysis (DSC)	32
3.3	Physicochemical properties analysis	34
3.3.1	Z-average.....	35
3.3.2	PDI	37
3.3.3	Zeta potential	39
3.3.4	Entrapment efficiency (%EE)	41
3.3.5	Relative drug loading (R-drug loading).....	42
3.4	Stability of the optimal formulations	44
3.5	LD release profile	46
3.6	Transmission electron microscopy.....	48
3.7	NLC containing BW, CA, PS and LD	49
4	Conclusions:	49
4.	Conclusão.....	80
5.	Bibliografia.....	82

6.	Anexos	88
6.1.	Artigos submetidos para publicação	88
6.2.	Anais de Congresso	88
6.3.	Declaração – Bioética e Biossegurança.....	92
6.4.	Declaração – Direitos autorais	93

1. Introdução

O presente trabalho encontra-se dividido em uma breve introdução teórica, seguido de capítulo redigido sob a forma de artigo, intitulado “Multilevel analysis to evaluate excipient-excipient interactions in the design of nanostructured lipid carriers”, e por fim conclusão do trabalho desenvolvido.

Sistemas de liberação modificada de fármacos

Os fármacos apresentam um intervalo de concentração terapêutica acima do qual são tóxicos e abaixo do qual são ineficazes. Como tentativa para manter a concentração do fármaco dentro do seu intervalo terapêutico por mais tempo, foram desenvolvidos os sistemas de liberação modificada de fármacos (*drug delivery system*, DDS) (Fig. 1). O DDS, além da função anteriormente descrita, permite ou objetiva o direcionamento do fármaco ao local desejado, diminuindo o número de doses, a toxicidade e os efeitos adversos e/ou colaterais. Por essas razões, a encapsulação de fármacos é de grande interesse científico, medicinal e comercial (KINGSLEY et al., 2006).

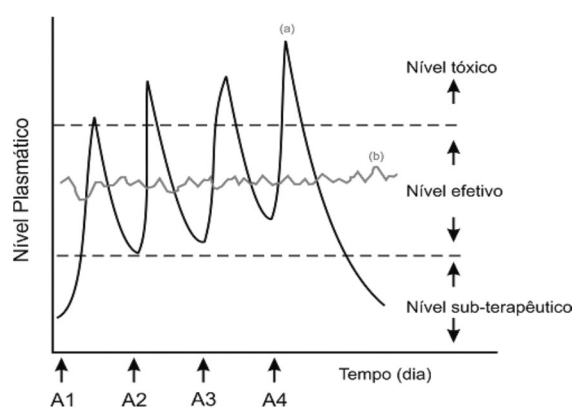


Figura 1. Comparação gráfica entre as variações de concentração de fármacos administrados por métodos convencionais de multidosagem (a) e sistema de liberação controlada (b), sendo A1, A2, A3 e A4 referentes a cada administração de uma dose do fármaco. Nota-se que no método (a) o nível plasmático se encontra diversas vezes fora do nível efetivo, enquanto o sistema (b) se mantém dentro do mesmo nível com apenas uma dose (DE LYRA et al., 2007).

Os DDS compreendem sistemas macroorganizados, como comprimidos, adesivos transdérmicos e géis, e sistemas micro/nanoestruturados, como complexos de ciclodextrinas, dendrímeros e sistemas poliméricos e lipídicos (GUTERRES; ALVES; POHLMANN, 2007). Dentre os DDS lipídicos coloidais, encontram-se os lipossomas, as nanopartículas lipídicas sólidas (Solid Lipid Nanoparticles, SLN),

carreadores lipídicos nanoestruturados (Nanostructured Lipid Carriers, NLC), conjugados lipídio-droga (CLD) e vesículas ou nanocápsulas lipídicas (NCL) (ATTAMA, 2011).

Os carreadores lipídicos podem ser classificados de acordo com o tipo de lipídio empregado e organização estrutural dessas moléculas. Esses sistemas apresentam como vantagens o fato de serem biocompatíveis, biodegradáveis e de terem flexibilidade em relação à natureza do fármaco encapsulado (GUSE et al., 2006).

Nanopartículas lipídicas – SLN e NLC

As SLN e NLC são sistemas coloidais lipídicos bastante explorados atualmente devido à sua baixa toxicidade, capacidade de alto carregamento de moléculas lipofílicas, capacidade de liberação sustentada do fármaco, produção escalonável, dentre outras propriedades. A Figura 2 ilustra esses dois tipos de nanopartículas, que são formadas por uma matriz composta por lipídio sólido (SLN) ou de estado físico misto sólido/líquido (NLC), considerando a temperatura ambiente e corporal. Essas estruturas são estabilizadas por emulsificante e dispersas em meio aquoso (ATTAMA, 2011; DAS; NG; TAN, 2012; PUGLIA; BONINA, 2012; SOUTO; ALMEIDA; MÜLLER, 2007; ZUR MÜHLEN; SCHWARZ; MEHNERT, 1998).

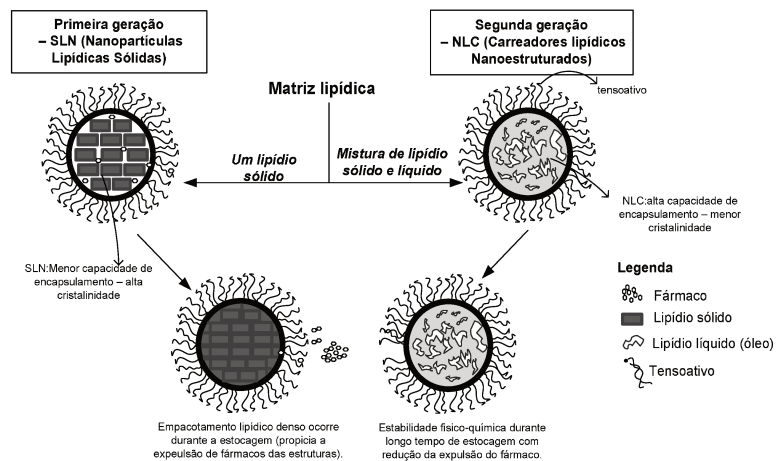


Figura 2. Representação e diferenças entre SLN e NLC. Extraído de De Araújo et al, 2013([DE ARAUJO et al., 2013](#)).

Os dois tipos de nanopartículas apresentam diâmetro médio de 50 a 1000 nm, podem ser usados por várias vias de administração (tanto tópica quanto oral e

parenteral), com excipientes biocompatíveis e de baixa ou inexistente toxicidade (MÜLLER et al., 1996). Como suas matrizes são compostas de triglicerídeos e ceras, são capazes de encapsular um percentual alto de fármacos com características hidrofóbicas e menos eficazes para carrear compostos com características hidrofílicas (MÜLLER; SHEGOKAR; KECK, 2011; PUGLIA; BONINA, 2012). Além das vantagens descritas, são relativamente estáveis fisicamente, sobretudo após o processo de liofilização por exemplo, que garante maior tempo de estocagem (ATTAMA, 2011; BATTAGLIA; GALLARATE, 2012; PUGLIA; BONINA, 2012).

Alguns pesquisadores (SCHWARZ; MEHNERT, 1999; ZUR MÜHLEN; SCHWARZ; MEHNERT, 1998) avaliaram a incorporação de fármacos lipofílicos (tetracaína, etomidato e prednisolona) em SLN, as quais apresentaram alta eficiência de encapsulação, perfil de liberação prolongado e manutenção do tamanho médio de partícula por longos períodos. No entanto, ocorre frequentemente a expulsão dos fármacos em função do tempo de estocagem, promovida principalmente pela presença de polimorfos lipídicos nas nanopartículas (WISSING; KAYSER; MÜLLER, 2004). Diante desse fato, foi desenvolvida uma segunda geração de carreador (NLC) que contém lipídio líquido em sua composição. Essa diferença resulta na redução do índice de cristalinidade da matriz lipídica, o que favorece o aumento da eficiência de encapsulação e diminui a expulsão do ativo durante a estocagem (PARDEIKE; HOMMOSS; MÜLLER, 2009; SAUPE et al., 2005).

Estabilização das nanopartículas lipídicas

De maneira simplificada, a estabilização de dispersões coloidais depende do equilíbrio das forças de gravidade/flutuação e de repulsão/atração. O desequilíbrio do primeiro conjunto pode causar sedimentação ou floculação; já a prevalência das forças de atração pode causar fusão, aglomeração ou dissociação das partículas. No caso das nanoemulsões, a desestabilização pode ainda causar a separação de fases do sistema; em todas as nanopartículas, qualquer um dos processos pode levar a estravazamento do fármaco para o meio externo (GANGULY; CHAKRABORTY, 2011; JIANG et al., 2010; STARK; PABST; PRASSL, 2010). Quando desestabilizada, a SLN sofre gelificação, fusão de partículas e perda de fármaco encapsulado. Tais eventos decorrem das alterações polimórficas dos

lipídios durante o armazenamento, não sendo resolvidos pela estabilização estérica dos tensoativos. Há dispersões otimizadas que retém a estabilidade física particulada, mas não necessariamente a eficiência de encapsulação (PARDESHI et al., 2012).

A diminuição da expulsão do fármaco pode ser atingida por uma combinação de excipientes e secagem, obtida por spray-drying ou por liofilização (FREITAS; MÜLLERÄ, 1998; VARSHOSAZ; ESKANDARI; TABBAKHIAN, 2012). Os excipientes podem tanto reduzir a cristalinidade da matriz como aumentar a solubilidade do fármaco (JENNING; MÄDER; GOHLA, 2000). Quando utilizada a secagem, a dificuldade de se manter um processo de spray-drying estéril favorece o uso de liofilização na aplicação de formulações parenterais (BONDÌ et al., 2014; JIA et al., 2010; LIU et al., 2008; VARSHOSAZ; ESKANDARI; TABBAKHIAN, 2012). A retirada da água em geral favorece a estabilidade no armazenamento e transporte, reduz o volume e peso por unidade e ainda possibilita armazenamento à temperatura ambiente de amostras que precisariam de refrigeração se diluídas (KONAN; GURNY; ALLÉMANN, 2002; LEE, 2003; LEE et al., 2009).

Caracterização físico-química das NLC

As nanopartículas são geralmente caracterizadas em função de sua distribuição de tamanho, carga superficial e morfologia, entre outras propriedades. O tamanho é calculado pelo diâmetro hidrodinâmico e acompanhamento de seu índice de polidispersidade (PDI), que reflete a distribuição dos tamanhos na amostra. A carga superficial é avaliada pelo potencial zeta (ZP), que é um potencial elétrico medido no plano de cisalhamento das nanopartículas. Altos valores de ZP em módulo indicam maior repulsão eletrostática entre as partículas e, consequentemente, maior estabilidade eletrostática das dispersões. Porém, quando as partículas são estabilizadas estericamente, o ZP não prediz estabilidade. Ainda, é importante a avaliação da forma das nanopartículas por microscopia eletrônica, que fornece imagens diretas das nanopartículas, podendo-se verificar a distribuição de seus tamanhos e formas (WU; ZHANG; WATANABE, 2011). No caso das NLC, também é adequado avaliar o grau de cristalinidade das matrizes lipídicas a partir de termogramas obtidos por DSC (Differential Scanning Calorimetry - Calorimetria Exploratória Diferencial), também relacionados com estabilidade (ATTAMA; MOMOH; BUILDERS, 2012).

Em relação ao dispersante, o parâmetro avaliado é o pH, sendo que variações nesse valor podem causar instabilidade das nanopartículas ou do fármaco carreado durante seu período de armazenamento (WU; ZHANG; WATANABE, 2011).

Anestésicos locais – lidocaína

Os anestésicos locais (AL) evitam ou aliviam a dor porque bloqueiam reversivelmente o processo de excitação das membranas de nervos periféricos. Assim, eles impedem a propagação do estímulo elétrico de forma a abolir a motricidade e sensações como tato e temperatura sem gerar perda de consciência, o que é inerente aos anestésicos gerais (COLLINS; WASHABAUGH, 1985; MALAMED, 2001; STRICHARTZ, 2008).

AL são moléculas anfipáticas, com a hidrofobicidade do grupo aromático (em uma das extremidades da molécula) e a polaridade conferida, em geral, por um grupo amino secundário ou terciário na outra extremidade da molécula; uma cadeia intermediária de caráter polar, éster ou amida, liga as extremidades (ARAÚJO; DE PAULA; FRACETO, 2008b; STRICHARTZ; RITCHIE, 1987). Os AL possuem pKa entre 7,6-8,9; o que implica que ambas as formas, protonada e neutra, estão presentes em pH fisiológico, com predomínio da protonada (MCLURE; RUBIN, 2005).

A estrutura e as propriedades físico-químicas são determinantes para a potência dos AL (ARAÚJO et al., 2003). A solubilidade aquosa, por exemplo, é essencial para o transporte e ionização dos AL, enquanto sua lipofilicidade garante que permaneçam nos neurônios, mantendo a nocicepção (BUTTERWORTH; STRICHARTZ, 1990). Todavia, os compostos anestésicos apresentam toxicidade diretamente proporcional à sua potência, o que se interpõe na busca de compostos mais ativos (ARAÚJO et al., 2003; DE PAULA et al., 2012).

As formulações atualmente comercializadas de AL possuem diferentes ativos, dosagens e formas farmacêuticas. Porém, a maioria proporciona tempo de analgesia limitado de, em média, quatro horas. Estratégias para aumentar o tempo de ação dos AL incluem a síntese de novos compostos ou o uso em associação medicamentosa (DE PAULA et al., 2010) com anti-hipertensivos (VAN TUIJL et al., 2006), anti-inflamatórios, vasoconstritores e opióides (QUEIRÓZ, 2012).

A lidocaína (LD), ou 2-(diethylamino)-N-(2,6-dimethylphenyl)acetamide, foi sintetizada pela primeira vez em 1954 e é a molécula pioneira dos AL do tipo amino amida (figura 3), sendo utilizada desde então como anestésico e analgésico local e antiarritmico (COLLINSWORTH; KALMAN; HARRISON, 1974).

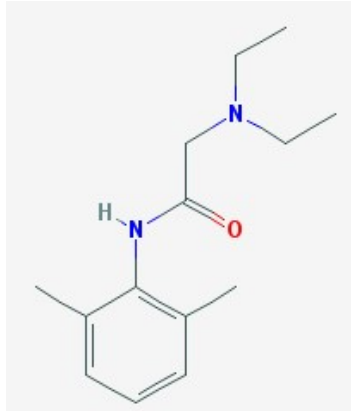


Figura 3. Estrutura química da lidocaína(PUBCHEM, [s.d.]).

No entanto, apenas recentemente estudos clínicos demonstraram que a administração intravenosa desse anestésico pode resultar em melhor controle da dor relacionada com câncer e pós-operatório imediato e tardio. Sua administração via intravenosa pode levar também a uma diminuição no consumo de opióides ou à substituição destes nos casos de pacientes refratários, sendo a melhora da dor mantida mesmo depois da eliminação do fármaco. Em adição ao efeito analgésico e hiperalgésico, a LD apresenta propriedades anti-inflamatórias, o que é desejável no tratamento pós-operatório. LD intravenosa é administrada como infusão ou diversos bolus devido a sua meia vida plasmática ser curta; essas condições requerem controles adicionais do paciente, equipamentos e/ou maiores doses do fármaco (GIBBONS et al., 2016; HERMINGHAUS et al., 2011; LAURETTI, 2008; MCCARTHY; MEGALLA; HABIB, 2010). Por isso, o desenvolvimento de um DDS de LD teria como vantagens o aumento no tempo de ação do AL, redução do número de administração do fármaco, com diminuição também no tempo de internação para tal administração, reduzindo-se assim a exposição de pacientes ao ambiente hospitalar e também aos custos envolvidos em uma internação.

Dada a importância dos DDS, as vantagens das NLC frente a outros tipos de carreadores e os benefícios que a LD poderia trazer quando encapsulada em sistemas de liberação modificada, o presente trabalho apresenta uma proposta de encapsular LD em NLC utilizando diferentes excipientes e utilizando um delineamento experimental e análise

estatística inovadores, que trazem como vantagens a possibilidade de observar interações entre os excipientes e fazer uma predição das quantidades mais adequadas de excipientes de acordo com as características físico-químicas observadas nos experimentos envolvendo as NLC. A metodologia proposta pode ser aplicada tanto para o *screening* de excipientes quanto para o desenvolvimento e otimização de formulações.

2. Objetivos

2.1. Objetivo Geral

Aplicar análise multiníveis no desenvolvimento de Carreadores Lipídicos Nanoestruturados (NLC) para encapsular lidocaína e verificação de interações entre os excipientes utilizados.

2.2. Objetivos Específicos

- Fazer *screening* de lipídios de acordo com seu potencial de solubilização da lidocaína;
- Determinar coeficiente de partição da lidocaína nos lipídios selecionados;
- Realizar delineamento experimental para avaliar o comportamento dos excipientes nas formulações desenvolvidas;
- Caracterizar físico-quimicamente as formulações desenvolvidas (diâmetro hidrodinâmico, índice de polidispersão, potencial zeta, eficiência de encapsulação, capacidade de carga);
- Determinar o perfil de liberação, morfologia e perfil térmico de formulações selecionadas a partir das características físico-químicas;
- Desenvolver metodologia de análise estatística dos resultados obtidos.

3. Capítulo I

Multilevel analysis to evaluate excipient-excipient interactions in the design of nanostructured lipid carriers

Viviane Lucia Beraldo-de-Araújo^{1,2,*}, Anderson Beraldo-de-Araújo³, Juliana Souza Ribeiro Costa^{1,2}, Ana Carolina Martins Pelegrine², Lígia Nunes Moraes Ribeiro², Eneida de Paula², Laura Oliveira-Nascimento²

¹*Department of Biochemistry and Tissue Biology, Biology Institute, State University of Campinas, Brazil, Rua Monteiro Lobato, 255, Campinas, SP, Brazil, Postal Code 13083-862;*

²*Pharmaceutical Technology Laboratory, Faculty of Pharmaceutical Sciences, State University of Campinas, Brazil, Rua Cândido Portinari, 200, Campinas, SP, Brazil, Postal Code: 13083-871;*

³*Center for Natural and Human Sciences, Federal University of ABC, Santo André, Brazil, Postal Code: 05508-090.*

* **Corresponding author:** Tel/Fax: +55 19 35218131. E-mail: vivi.beraldo@gmail.com.

ABSTRACT

To rationally formulate nanoparticles, it is crucial to know the interaction among their excipients and how they change physicochemical attributes of nanoparticles. This is especially critical for the screening and development of nanostructured lipid carriers (NLCs) because they are made of at least three types of excipient (solid lipid, oil and surfactant). Exhaustive combinations of excipients and comparisons to assess their influence on the design of NLCs have been performed, but with no practical perspective to quantify synergistic interaction of NLCs components. In this article, we propose an innovative approach to analyze the effect of excipient interactions on physicochemical properties of NLCs. It compasses two sequential experiments with Hall design, mathematical modelling with mixed models and multilevel statistics. NLCs were prepared by hot emulsification-ultrasonication method. The inputs of NLCs analysis were lidocaine as the hydrophobic model drug and nine excipients; the outputs were z-average (size, measured by Dynamic Light Scattering, DLS), polydispersity index (PDI, measured by DLS), zeta potential (DLS), entrapment efficiency (HPLC) and drug loading of NLCs (HPLC). All the linear regression models for the experiments exhibited good effect values with significant F-statistics ($p =$

0.01). For all outputs, the second experiment permitted higher fitting than the first one, with significant F-statistics ($p = 0.02$). This allowed evaluating the interactions based on the models of the second experiment. Hence, castor oil (CA), cetyl palmitate (CP), capric/caprylic acid (CC) and polysorbate 80 (PS) presented larger effects among the excipients as well as a clear pattern of synergistic interactions among them. To confirm some of the outcomes, a NLC made of beeswax (BW), CA, PS and lidocaine was analyzed and exhibited the predicted pattern of the physicochemical characteristics. This shows the robustness of the methodology, which can be applied not only to NLCs but also to the production of other nanoparticles.

KEYWORDS: Multilevel statistical analysis; Design of experiment; NLC; Nanostructured lipid carrier; natural lipids; lidocaine

1 introduction:

Nanostructured lipid carriers (NLCs) are the second generation of solid lipid nanoparticles (SLN), widely used as biodegradable and safe delivery systems for hydrophobic drugs and bioactive substances ¹⁻³. They are submicron particles of a mixed solid-liquid lipid core coated with surfactants; the carried substance is generally located within the lipid core. In order to obtain reproducible and stable NLCs, they should present low polydispersity index of particle size, high zeta potential in module and high encapsulation efficiency ⁴.

To manipulate these properties, one could alter critical process parameters or formulation parameters. Formulation critical parameters of NLCs include the lipid type, amount, crystallinity and melting point, besides drug and surfactant properties ⁵. Therefore, to perform a rational formulation design, it is crucial to know which excipients interact with each other and change the physicochemical attributes. Some researchers have done exhaustive combinations of excipients and comparisons to assess both qualitative and quantitative influences of the investigated factors for NLCs. Although they reported the presence of synergistic interaction of the components of NLCs, with respect to physicochemical outputs, they did not quantitatively approach the subject. In fact, these several combinations of excipients have been analyzed with small and isolated experimental full designs, which do not

allow to investigate synergistic interactions because the factors of each isolated experiment are different^{6–10}.

We present in this article, for the first time, a method to analyze the interactions of the excipients with respect to the physicochemical properties of NLCs. The method begins with pre-formulation studies, to evaluate the viability of excipient combinations. In the second stage, we implement two sequential experimental Hall's design to have a mixed model of the excipient interactions. Hall's design is a non-regular design that permits to combine up to 15 factors with just 16 runs, with no full aliasing among them and their two-factor interactions. In contrary, regular strategies depend on a large amount of samples, such as full factorial designs, not always feasible. Also, in models with few samples, a greater uncertainty arises and the effect of a single substance is confounded with two factor interactions. After performing the experiments, we assess the physicochemical characteristics of NLCs (z-average, polydispersity index, zeta potential, entrapment efficiency and drug loading). To evaluate the variance along the two experiments, multilevel analysis is applied, and then there are formulated linear models of the main and interactions effects. Next, we apply Wu-Hamada's definition of conditional effects¹¹ to build graphs of the excipients synergy. The third step is the formulation studies. This stage aims to understand the reasons and consequences of the verified interactions (formulations stability, release profile of the model drug and transmission electron microscopy). The summarised workflow is represented in Fig. 1.

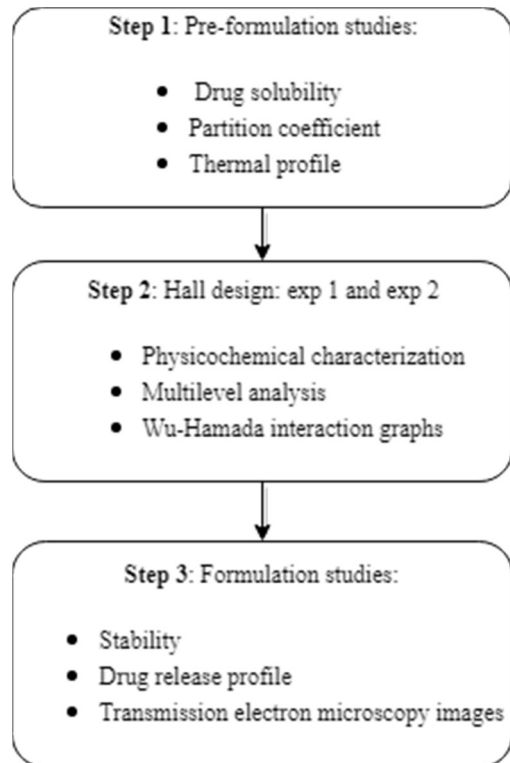


Figure 4. Workflow of the developed methodology.

In what follows, we report the outcomes of the application of this method to a NLC-loaded lidocaine as the hydrophobic model drug. Five natural liquid lipids (castor, sesame, cottonseed, corn, and capric/caprylic oils) were compared together with two natural solid lipids (beeswax and cetyl palmitate) and two surfactants (poloxamer 188 and polysorbate 80). In our method, the levels of excipients are changed directly; therefore, we get mixed models of the main factors and their interactions. For this reason, the present work allows us to refine previous results in the literature about the interaction among the NLC excipients, as well as to predict new effects that were not previously reported. From a practical viewpoint, it permit us to apply systematic criteria to choose the excipients to develop NLCs and provide guideline for formulations of NLCs based on the analysis of interaction among their excipients, which is applicable not only to this, but also to other drug delivery systems.

2 Methods:

2.1 Material

Super Refined™ excipients were gently donated by Croda do Brasil: castor oil (CA), sesame oil (SO), cottonseed oil (CS), corn oil (CO), polysorbate-80 (PS), beeswax (BW); Crodamol™CP-PA (CP). Liponate® GC (Capric/caprylic oil, CC) was gently donated by Lipo do Brasil. Poloxamer 188 (Kolliphor® 188, KO), acetonitrile and lidocaine (LD) base were purchased from Sigma.

2.2 Lipids selection

The previous selection of lipids was according to the following features: natural origin, theoretical capability to solubilize lidocaine, melting point and availability of highly purified samples. The chosen melting point range for solid lipids was 45 to 70°C (selecting cetyl palmitate and beeswax), to guarantee the solid state in room or body changes in temperature and preserve drug integrity upon heat degradation ¹⁴. The chosen melting point range for liquid lipids was below 0°C to guarantee the liquid state in room/refrigerator changes in temperature (selecting castor, sesame, cottonseed, corn, and capric/caprylic oils). The maintenance of the original physical states assure that these physical transitions do not interfere with physicochemical outcomes among different formulations, masking possible interaction effects. Liponate GC® is not a super refined oil, but we kept it as a gold standard, since it is the most used liquid lipid to produce NLCs ¹⁵.

2.3 Lidocaine solubility

The solubility of lidocaine was evaluated as reported previously (adapted method described by Joshi and Patravale ¹⁶). Briefly, increments of 10 mg LD were added into 500 µL of oil until there were no complete solubility of the added amount. To assess the solubility in solid lipids, increments of LD were added to 50 mg of melted solid lipid and determination was visual.

2.4 Partition coefficient of lidocaine

The partition coefficient ($\log P$) of lidocaine in lipids was determined by adding 10 mg of the drug into a mixture of 3 mL of water and 3 mL of lipid and mixed along 24 hours. After that, the aqueous phase was obtained through centrifugation (5000 rpm, 10 minutes) and filtered (0,45 μm pore membrane). LD determination in aqueous phase was obtained in HPLC (refer to quantification of LD method)¹⁷. The determination of LD in oily phase was done by the difference between the LD added and LD in the aqueous phase. Partition coefficient was calculated according to Eq. (1). (1)

2.5 Preparation of Nanostructured Lipid Carriers (NLC)

NLC were prepared using hot emulsification-ultrasonication method¹⁸. Briefly, lipid phase was melted in water bath 10 °C above the melting point of the solid lipid, followed by addition of LD under magnetic stirring up to complete homogenisation. In another beaker, aqueous phase was heated under magnetic stirring and dropped into lipid phase under high-speed agitation (1200 rpm for 3 min in ultra-turrax blender (IKA® T18 basic, Staufen, Germany)). After that, the emulsion was submitted to tip sonication (Vibracell, Sonics & Materials Inc., Danbury, USA), operated at potency 130 W, frequency 20 kHz and amplitude 50 % in cycles of 30 seconds (on/off) during 30 minutes. The formulation was cooled in ice bath until reach room temperature and stored at room temperature.

2.6 LD Quantification, entrapment efficiency and drug loading:

The entrapment efficiency (%EE) of LD into NLC was determined indirectly by ultrafiltration method using centrifugal filter tubes (Millex, Millipore, Bedford, MA, USA) with a 30 kDa molecular weight cut-off. NLCs suspensions were centrifuged at 18514 x g, during 20 min. %EE was calculated by the difference between the amount of LD in the formulations and the amount detected in the filtrate, applying the Eq. (2)^{19,20}: (2).

Assay of LD was performed by HPLC as described in its USP monograph²¹, with the Waters Breeze 2 HPLC system (Waters, Milford, Massachusetts, USA). The parameters were: UV detection at 254 nm (detector UV 2998 waters); mobile phase

with 4 parts of glacial acetic acid 0.5 % in deionized water, pH 3.4 and 1 part of acetonitrile; flow rate of 1.5 mL/min; injection volume of 20 µL; column NST 18 – 300 mm x 3.9 mm x 4 µm (L1); 10 minutes of running time. Drug loading (%DL) was calculated by Eq. (3): (3).

To analyze the results of %DL there were calculated the relative drug loading (%RDL), comparing to the theoretical drug loading (Eq. (4)): (4), where theoretical %DL is obtained considering the total amount of LD added. We use the relative drug loading because the samples have different amounts of the excipients and LD, so it is necessary to scale the data to compare them appropriately.

2.7 Determination of hydrodynamic diameter (z-average), polydispersity index (PDI) and zeta potential (ζ)

The z-average was determined by Dynamic Light Scattering (DLS) (Zetasizer Nano ZS, Malvern Instruments Ltd, Malvern, England), at 90° angle and 25 °C, with samples diluted 1:200 in ultrapure water (refraction index 1,333 – viscosity 0,8905 cP) for adequate correlation coefficient (between 0,7 - 1). Zeta potential was determined by electrophoretic mobility in the same instrument.

2.8 Differential Scanning Calorimetry (DSC)

DSC thermograms of the bulk materials and NLCs samples were obtained using a Mettler instrument model DSC1 (Mettler-Toledo Schwerzenbach, Switzerland). The samples were weighted on microanalytical balance Metler Toledo, model MX5 (Mettler-Toledo Schwerzenbach, Switzerland). Blanks were automatically deducted. For analysis, the parameters were aluminum pans, temperature range of 20–80 °C, heating rate of 5 °C per minute, N₂ atmosphere (50 mL per minute).

2.9 LD in vitro release profile

The release of LD was analyzed in a Franz diffusion cell system, in which a dialysis membrane with a molecular exclusion pore size of 14 kDa separate the donor (1 mL of sample) and acceptor (12 mL of phosphate buffer pH7.4) compartments. The cell were kept at 37 °C and under magnetic stirring (300 rpm)²². 200 µL of each sample in each time point were withdrawn from the acceptor

compartment for LD quantification; the same withdrawn volume was replaced by buffer to maintain the total cell volume.

2.10 Transmission electron microscopy

Transmission electron microscopy (TEM) was used to evaluate morphology, integrity and size of NLC. There was added uranyl acetate (2 %) to the appropriately diluted NLC to provide contrast, after which aliquots were deposited onto copper grids coated with a carbon film and dried at room temperature. After drying, micrographs of the samples were obtained using a JEOL1200 EXII microscope operated at 80 kV²².

2.11 Design of Experiment (DoE) and statistical analysis

The DoE used was the first 10 columns of the Hall's design²³. As a non-regular design with two levels, it permits to combine up to 15 factors in 16 runs, without full factor aliasing²⁴. In this work, we used 10 factors: 9 excipients and one drug model. The experimental plan consisted in two sequential Hall's designs to have a mixed model of the interactions among the excipients (STables 1 and 2). Lidocaine was used as a drug model, so its levels were fixed in both designs. To make general conclusions about the action of the solid and liquid lipids, as well as the surfactants, their levels were changed from the first to the second experiment.

The statistical analysis was performed with the language R²⁵. At first, there was assessed the variability between the two experiments via the maximum-likelihood estimation (Cf. GLS and IMM models in Supplementary Material). Next, a linear model (GM) for the data of both experiments was generated with the step-by-step method, and validated with a multilevel analysis (Cf. GM and FMM in Supplementary Material). Thus, GM was used as models (M1 and M2) for each experiment separated, to analyze its representability of each experiment. To evaluate the complex confounding of two-factor interactions and main effects of Hall's design, we applied Wu-Hamada's definition of conditional effects¹¹ to the model (M1 or M2) that presented highest R² and significative F-statistics – the significant factors and interactions was validated by the final multilevel model FMM.

The statistical assumptions of the models generated were all of them tested (Cf. Supplementary Material). The normality of the residuals was assessed by Shapiro-Wilk test. For the independence of the errors, it was used the Durbin-Watson test. Homoscedasticity was assessed with Breusch-Pagan. The analysis of the influence of the samples was made with Cook's distance and hat-values, and collinearity of coefficients with the variance inflation factor (VIF). Finally, confidence interval was checked^{26,27}.

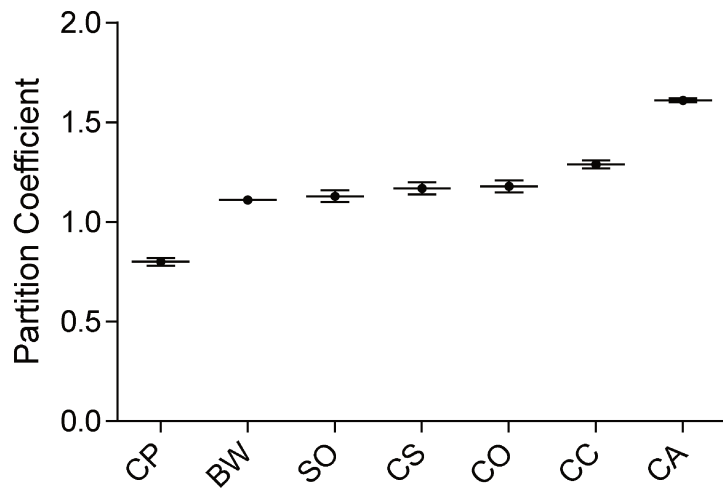
3 Results and discussion:

3.1 LD solubility and partition coefficient:

The evaluation of selected lipids and surfactants was according to their ability to solubilize LD (Fig. 2.A). All liquid lipids solubilized more than 100 mg/mL of LD, and all solid lipids solubilized more than 0,2 mg/mL of the drug; both mass proportion are the minimum mass levels proposed in our DoE, therefore it is guaranteed that LD would be able to fully solubilize in both lipid types, decreasing risk of drug crystallization. Surfactants increased LD solubility in water at least two-fold. According to USP solubility definition, LD was very soluble in solid lipids, freely soluble in oils and slightly soluble in water and surfactants²⁸. Solubility of LD presented the following order: liquid lipids: CA=CC > SO=CO > CS; surfactants: PS > KO; solid lipids: BW > CP.

Excipient	Solubility
<i>Solid lipids (mg/mg)</i>	
BW	7
CP	4
<i>Oils (mg/mL)</i>	
CA	260 - 280
CC	260 - 280
SO	160 - 180
CO	160 - 180
CS	120 - 140
<i>Surfactants and water (mg/mL)</i>	
PS 1%	5
KO 1%	4
Deionized water	2

(A)



(B)

Figure 5. A. Solubility of lidocaine (LD) in the excipients (BW=beeswax, CP=cetyl palmitate, CA=castor oil, CC=capric/caprylic oil, SO=sesame oil, CO=corn oil, CS=cottonseed oil, PS 1% = polysorbate 80 1% (V/V) in water, KO 1% = poloxamer 188 1% (w/V) in water). The solubility range of LD in oils is due the method of determination and means the amount that solubilize (low number) and the amount that is not completely soluble in each oil (higher number). **B.** Partition coefficient of LD in solid and liquid lipids (average \pm standard deviation). The experiment was ran in duplicate.

The partition coefficient (Fig. 2.B) agrees with the solubility profile, in the sense that lipids with higher or lower LD solubility also presented higher and lower partition coefficients, respectively. Partition coefficient of LD presented the following order: CA > CC > SO=CO=CS=BW > CP. Differences between measurements of intermediate excipients might be due to solubility determination method, which resulted in ranges rather than exact values. However, for our purpose, ranges are adequate to guarantee solubility in NLCs.

3.2 Thermal analysis (DSC)

The thermal analysis (Fig. 3) showed the purity of CP, whereas its melting peak is characteristic of a β polymorph, the most stable crystalline form of lipids². LD also

presented a narrow melting peak, which indicates purity and identification, according to the range determined by USP²¹. BW presented a large peak because it is a complex mixture of organic compounds, and its composition varies depending on the genetic characteristics of the bees, as well as the site of collection. Also, its melting point is in accordance to the literature range⁹. NLC presented peaks in two different regions: one in 58.89 °C, which may represent the BW, and another one in 67.77 °C, that probably corresponds to LD that was not encapsulated. Thermal analysis of liquid lipids were not performed because they present no significant changes on their behavior in the range of temperature evaluated.

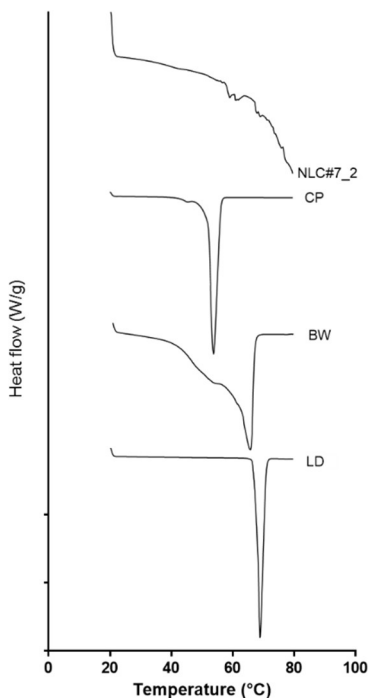


Figure 6. Thermal analysis (DSC) of the solid lipids (CP and BW), LD and NLC#7_2 (from experiment 2). LD has a narrow peak, as well as CP, in 68.87 °C and 53.82 °C, respectively. BW presented a broad peak in 65.7 °C, and NLC#7_2 mainly two peaks, in 58.89 and 67.77 °C. Analysis was carried out increasing the temperature from 20 to 80 °C, heating rate of 5 °C per minute, N2 atmosphere (50 mL per minute).

Table 1 presents the thermodynamics characteristics of the excipients and formulation analyzed by DSC.

Table 1. Summary of DSC analyses (melting point of solid bulk materials/ NLC).

Sample	Integral (mJ)	Integral/weight (J/g)	Onset (°C)	Peak (°C)
NLC#7_2	-32,76	-3,5	57,71	58,89
	-15,08	-1,6	67,05	67,77
LD	-525,81	-66,7	67,58	68,87
CP	-1050,39	-195,7	52,04	53,82
BW	-780,83	-145,5	59,6	65,7

3.3 Physicochemical properties analysis

The statistical analysis of the data from experiments 1 (exp 1) and 2 (exp 2) were performed, considering the z-average, PDI, zeta potential, entrapment efficiency and relative drug loading. Exp 1 differs from exp 2 in the levels of some factors (STables 1 and 2, from Supplementary Material), which allows inferences about excipient interactions in intervals of values and not only fixed combinations of levels, as it is usually made in fixed models.

All the responses, except PDI ($p<0.05$), did not present significative intercept variance from exp 1 to 2 ($p>0.9$). All the linear regression models for the experiments together exhibited good effect size ($R^2 >0.61$) with high significative F-statistics ($p<0.01$). In special, the global model when applied to exp 2 always presented higher fitting ($R^2 >0.82$) than the exp 1 and with significative F-statistics ($p<0.02$). Since the multilevel analysis confirmed that the global linear model was very significative for each response ($p<0.001$), we could analyze the interactions directly in the data of the models of exp 2.

The resume of the results that will be discussed in this section is the following. Z-average (ZA) presented unimodal distribution, mean size (322 ± 47) nm. The interaction between polysorbate-80 (PS), castor oil (CA) and cetyl palmitate (CP) determined ZA. Polydispersity index (PDI) variated between 0.14 to 0.35, mean (0.23 ± 0.05). The main factors that influenced PDI were PS, CP and CA. Zeta potential (ZP) presented mean value (-46.2 ± 4.4) mV. Surfactants presented divergent performance on ZP, due to interactions with liquid lipids. Entrapment efficiency was between 58 % and 79 %, mean (72 ± 5) %, and relative drug loading from 60 % to 80

%, mean (70 ± 5) %. For both, the interaction among liquid lipids was crucial, such as cottonseed (CS) and capric/caprylic (CC) oils.

3.3.1 Z-average

Fig. 4 (a) shows the behavior of z-average along the two experiments.

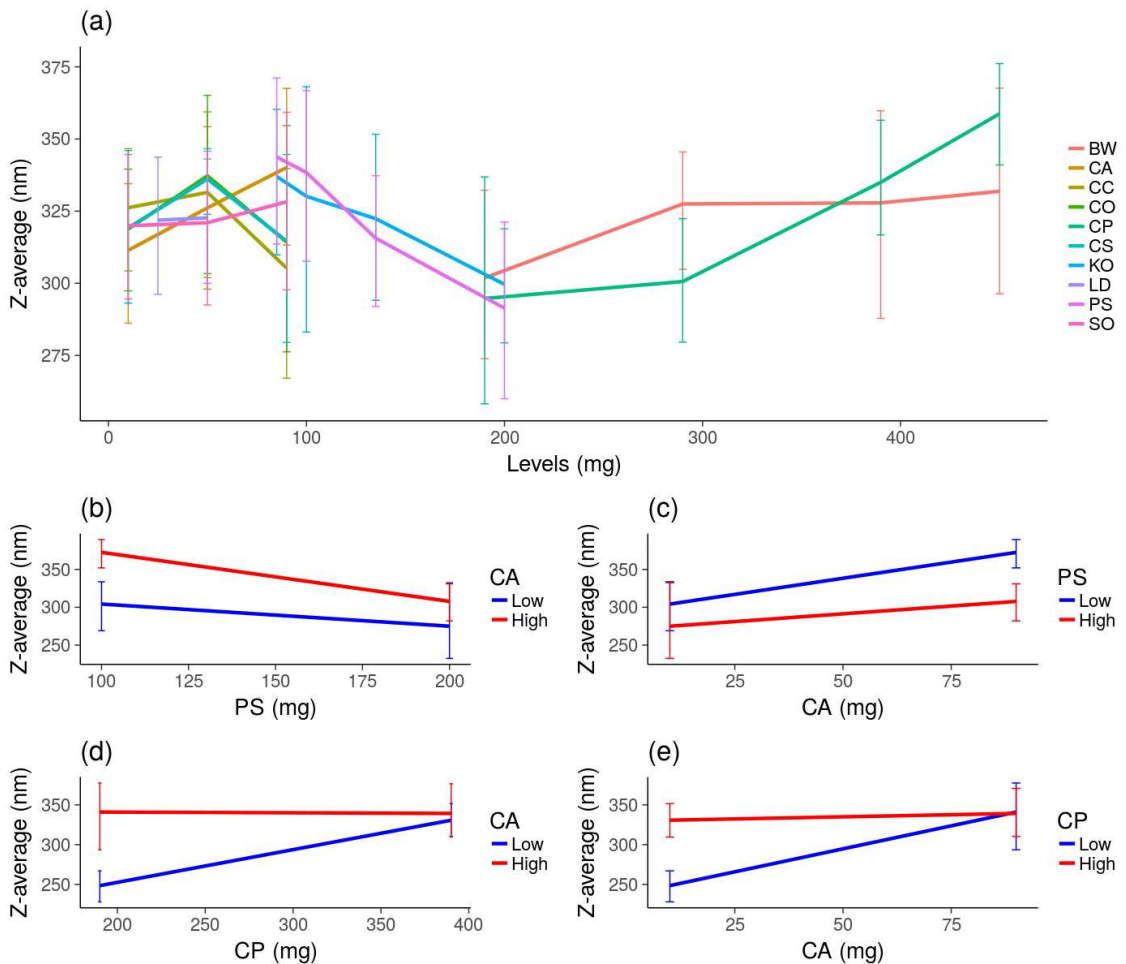


Figure 7. Z-average distribution from exp 1 and 2 at low and high levels of each excipient (BW= beeswax, CA= castor oil, CC= capric/caprylic oil, CO= corn oil, CP= cetyl palmitate, CS= cottonseed oil, KO= poloxamer 188, LD= lidocaine, PS=polysorbate 80, SO= sesame oil). Error bars correspond to the standard deviation of samples mean of each experiment. The values of levels of each experiment are in STables 1 and 2 (a); interaction of PS on CA in z-average of exp 2 (b); interaction of CA on PS in z-average of exp 2 (c); interaction of CP on CA in z-average of exp 2 (d); interaction of CA on CP in z-average of exp 2 (e).

It is clear, and in accordance to the literature, that the solid lipids act to increase the z-average (Fig. 4 (a)), with emphases for CP ($p<0.0001$). Some authors also

described this comportment of CP on the NLC particle size, claiming that the viscosity of the lipid phase increases at high CP concentrations, which affects the homogenisation during NLC production via hot homogenisation method, allowing the aggregation of the particles and increase of particle size^{4,9}.

Contrary to solid lipids, the increase in surfactants amounts decreased the z-average (Fig. 4 (a)). Their action is collinear, PS has a prominence but neither PS nor KO had significant effects alone, only in interaction with other excipients. Fig. 4 (a) also shows that liquid lipids are almost confounded, and according to Teeranachaideekul¹⁰, the oil content did not affect the mean particle size. The exception is CA: it increased the z-average ($p<0.0001$), and this action may be explained by Hu *et al*²⁹, where they stated that smaller nanoparticles are obtained from the use of less viscous oils (and CA was the most viscous oil that we used). The multilevel analysis revealed that the prominence of PS was an effect of its interaction with CA ($p<0.01$). Fig. 4 (b) displays this interaction. CA in its highest level made an increase in the z-average (Fig. 4 (c)). On the other hand, when PS was in the high level, the z-average was smaller (Fig. 4 (b)). In accordance with Fig. 4 (a), PS on both levels of CA decreased the z-average (Fig. 4 (b)), and CA on both levels of PS increases z-average (Fig. 4 (c)). Helgason *et al*³⁰ described that the increase in the particle size of SLN was accentuated with low surfactant concentrations (they worked with 10% of solid lipid and a variation between 1 – 5 % of tween 20 (w/w)). According to them, this occurs because the surface of the particle is less covered with the surfactant and, therefore, there is an increased probability to happen particle-particle interactions. Our results about the interaction between PS and CA shows that this is not what happened for NLCs, considering the tested lipids. At least in the cases analyzed in our experiments, the effect of the surfactants is associated to their interactions with the liquid lipids. To provide an explanation for this phenomenon, further studies are necessary.

Lastly, the interaction between CA and CP also was significant ($p<0.05$). Separated, when either CA or CP were at high levels, both maintained elevated values of z-average, and reached low values of z-average when both were at low levels. In addition, when some of them was at a low level, the other one acted to increase the z-average (Fig. 4 (d) and (e)).

This analysis indicates that to choose among the levels of each factor, it is necessary to consider the applicability of the formulation and its desirable size. For example, if one is developing a NLC to a parenteral application, it is necessary that NLC is between 100 – 200 nm¹⁴. Considering this, according to the described multilevel analysis of z-average, there were desirable to choose CP and CA in low levels, and PS in high levels.

3.3.2 PDI

Fig. 5 (a) shows that the behavior of PDI along the two experiments was different ($p<0.05$). With respect to the liquid lipids, it is possible to visualize that at higher levels, they tended to raise the PDI in the exp 1 but to decrease in the exp 2, which has higher amounts of lipids. The same happened to solid lipids, but not so much pronounced.

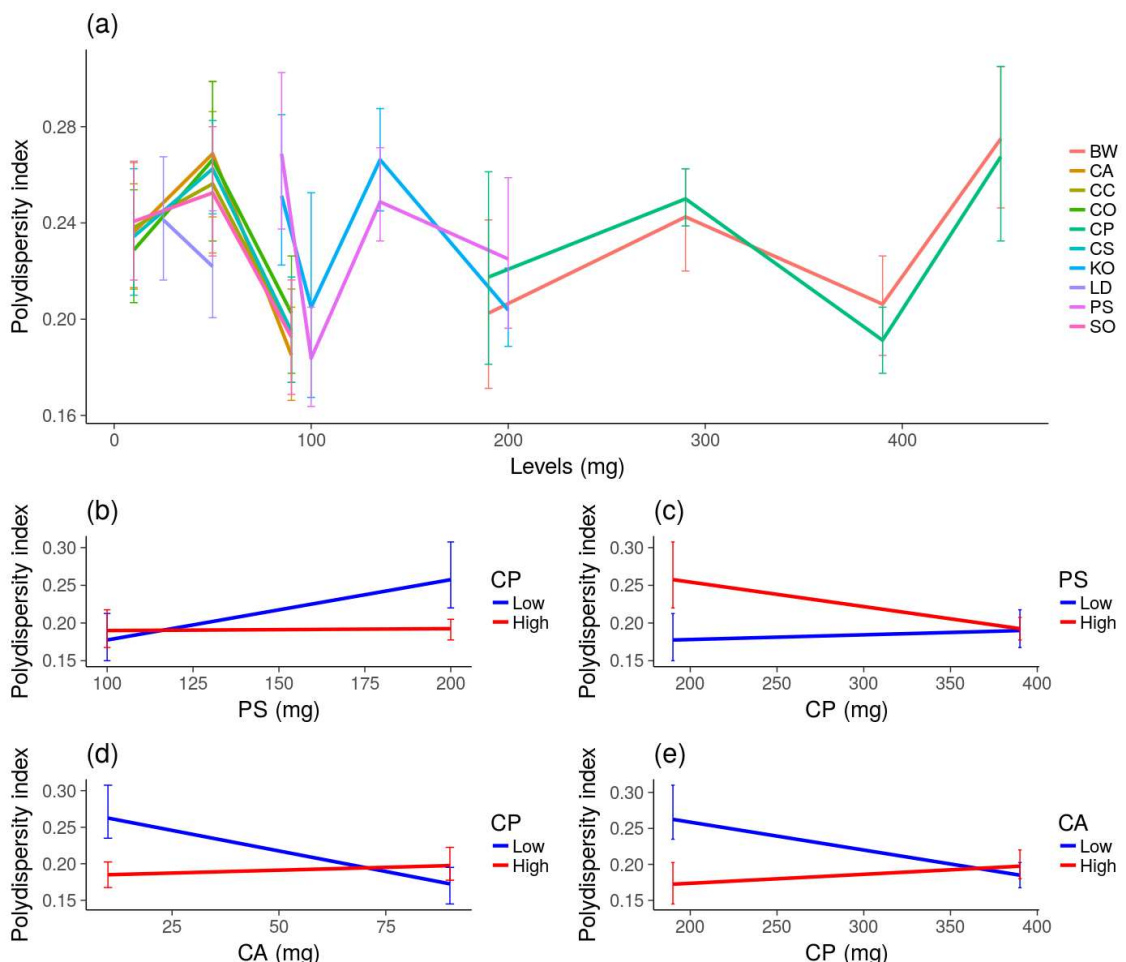


Figure 8. Polydispersity index (PDI) distribution from exp 1 and 2 at low and high levels of each excipient (BW= beeswax, CA= castor oil, CC= capric/caprylic oil, CO=

corn oil, CP= cetyl palmitate, CS= cottonseed oil, KO= poloxamer 188, LD= lidocaine, PS=polysorbate 80, SO= sesame oil). Error bars correspond to the standard deviation of samples mean of each experiment. The values of levels of each experiment are in STables 1 and 2 (a); interaction of PS on CP in PDI of exp 2 (b); interaction of CP on PS in PDI of exp 2 (c); interaction of CA on CP in PDI of exp 2 (d); interaction of CP on CA in PDI of exp 2 (e).

Rose et al (2015) verified that increasing the total amount of lipids affected positively the PDI, probably due to the elevation in lipid concentration ³¹. Our multilevel analysis showed that the factors that influenced the z-average were also the ones that influenced PDI, namely, the main effects of PS (to increase, p<0.0001) and CA (to decrease, p<0.01). In Fig. 5 (b), we see the interaction between PS and CP (p<0.01). If CP is at high level, PS has no effect, but when CP is low, PS increases the PDI (Fig. 5 (b)). Contrarily, if PS is at high level, CP decreases the PDI, but has no effect if PS is low (Fig. 5 (c)). This general behavior that the high amount of lipids and low amount of surfactant decreases PDI was reported by Martins *et al* ⁷. Thus, as we presented, the relationship among the lipids, at least with respect to the solid ones, and surfactants is not immediate, because it depends on the level of each factor. Fig. 5 (d) and (e) make this point. If CP is at high level, CA has no effect, but when CP is low, CA decreases the PDI (Fig. 5 (d)). On the other hand, if CA is at high level, CP has no effect to the PDI but CP decreases it if CA is low (Fig. 5 (e)). Therefore, combining these results, we have that CP, CA and PS interacted all of them in non-trivial ways. This shows that Gonzalez-Mira *et al* ³² assertion that surfactants alone can contributed to lower PDI values is not a general rule. They conclude it (studying poloxamer 188) because their inputs were proportions of total lipids and surfactants, which do not provide information about interactions among the excipients that our analysis can provide.

The multilevel analysis also showed that BW and the interaction between BW and CP were significant (p<0.001), but their effects were smaller when compared to those analyzed above.

As it is always desirable to obtain low PDI values, and considering that the most influent excipients were CA, PS and CP, the results suggest keeping CA and CP at highest levels and PS at lowest levels. However, an accurate analysis must be done whenever the levels of the factors indicate opposite solutions to obtain the desirability criteria. For instance, in a first analysis, to obtain a small NLC, low amount of CP is

required. However, to obtain low PDI value, it requires high amount of CP. Then, to define CP amount, it is important to check whether CP is a main factor or if it is actually interacting to another excipient. In the PDI, CP is not acting alone, therefore we can use it at low levels as soon as we keep PS also at low levels (cf. Fig. 5 (b) and (c)), and CA at high levels (Fig. 5 (d) and (e)).

3.3.3 Zeta potential

Fig. 6 (a) presents the influence of excipients on zeta potential. Despite the consistent trend of the solid lipids to increase the zeta potential in module, their effect was not significant. On the other hand, the liquid lipids CA ($p<0.01$) and CS ($p<0.05$) acted to make the zeta potential more positive. The effect of the amount of oils on the zeta potential values may be associated to the disruption of the surfactant shell promoted by the high concentration of liquid lipid, which leads a rearrangement of the surface charge of the nanoparticles^{9,33}. In addition, PS increased the zeta potential ($p<0.01$), and from Fig. 6 (a) it seems that KO presented the same action.

It was reported by Ribeiro *et al*^{8,22} that the interaction among solid and liquid lipids with poloxamer 188 has different effects on the zeta potential depending on the natural lipids used (copaiba oil, beeswax, sesame oil, and others). Here we can make this assertion precise with respect to both surfactants. Fig. 6 (b) and (c) show that KO and CA have a simple synergistic interaction ($p<0.01$): at both levels of each other, low or high, they acted to decrease the zeta potential (more negative). This explains the action of the KO: CA acted to make the zeta potential more positive, and so the same happened to KO. On the other side, PS significantly interacted with LD ($p<0.0001$).

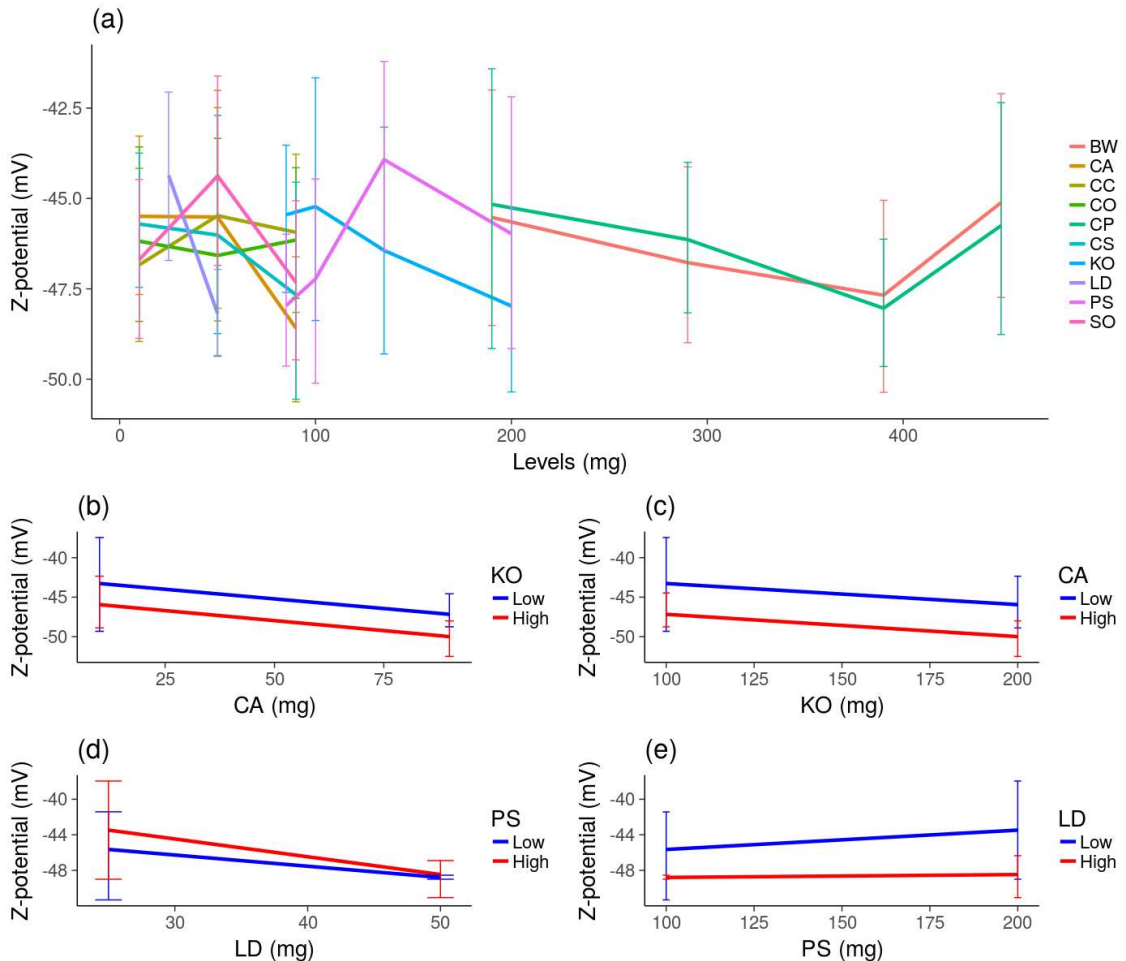


Figure 9. Zeta potential (ZP) distribution from exp 1 and 2 at low and high levels of each excipient (BW= beeswax, CA= castor oil, CC= capric/caprylic oil, CO= corn oil, CP= cetyl palmitate, CS= cottonseed oil, KO= poloxamer 188, LD= lidocaine, PS=polysorbate 80, SO= sesame oil). Error bars correspond to the standard deviation of samples mean of each experiment. The values of levels of each experiment are in STables 1 and 2 (a); interaction of CA on KO in ZP of exp 2 (b); interaction of KO on CA in ZP of exp 2 (c); interaction of LD on PS in ZP of exp 2 (d); interaction of PS on LD in ZP of exp 2 (e).

In Fig. 6 (d), we can see that LD at both levels of PS turned the zeta potential more negative, and so contributed to the stability of the NLC. On the other hand, in Fig. 6 (e), we observed that when LD is at high level the zeta potential is very negative, and PS has no effect, but when LD is at low level the zeta potential is less negative and PS contributes to increase it. Moreover, the model generated for the zeta potential response shows that PS interacted significantly with CS ($p<0.01$) and CC ($p<0.01$), but the size of the effect of these interactions were not big as the interaction with LD.

Once all the formulations reached good zeta potential values (higher than 30 mV, in module), it is not necessary to restrain the levels of the factors that contributed to influence this output. Nonetheless, our results show that the interaction of the surfactants with the liquid lipids is relevant to understand the behavior of the zeta potential. It is also important to mention that LD, as a drug model, contributes to stabilize the NLC, probably because it interferes the superficial composition of the nanoparticles.

3.3.4 Entrapment efficiency (%EE)

In Fig. 7 (a) we can see that PS ($p<0.05$) and CS ($p<0.01$) increased the %EE. Although Fig. 7 (a) does not make clear the action of CC and SO, multilevel analysis indicated that CC ($p<0.01$) and SO ($p<0.01$) decreased %EE.

Another fact is that the liquid lipids interacted with the other excipients to determine the entrapment. In special, the interactions between CC and CS was very significant ($p<0.001$). In Fig. 7 (b) it is clear that CS has no effect on the levels of CC, and the entrapment is directly proportional to the level of CC. This is confirmed in Fig. 7 (c), where CC increased the entrapment independently of the level of CS. The interaction between SO and KO also was significant ($p<0.01$). Figs. 7 (d) and (e) show that SO and KO had action similar to CC and CS. This behavior was covered by Pathak *et al*⁵, where they stated that the increase in entrapment is dependent not only on the solubility of the drug in the carrier, but also on the amount of liquid lipid⁵.

An interesting point is that PS exhibited many interactions with respect to %EE: it interacted with CC ($p<0.001$), CO ($p<0.01$) and KO ($p<0.01$), but the size of the effect of these interactions was less grandiose than the reported ones.

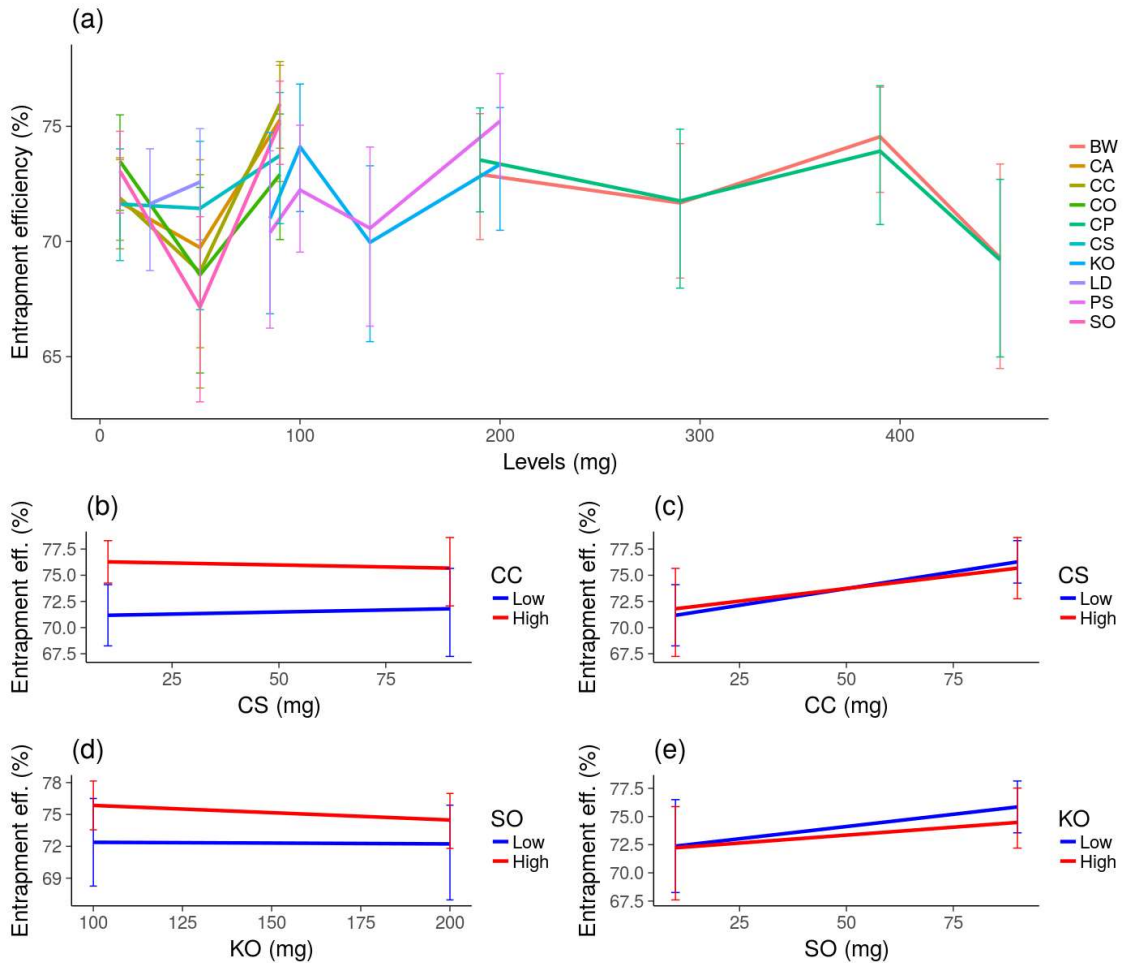


Figure 10. Entrapment efficiency (%EE) distribution from exp 1 and 2 at low and high levels of each excipient (BW= beeswax, CA= castor oil, CC= capric/caprylic oil, CO= corn oil, CP= cetyl palmitate, CS= cottonseed oil, KO= poloxamer 188, LD= lidocaine, PS=polysorbate 80, SO= sesame oil). Error bars correspond to the standard deviation of samples mean of each experiment. The values of levels of each experiment are in STables 1 and 2 (a); interaction of CS on CC in %EE of exp 2 (b); interaction of CC on CS in %EE of exp 2 (c); interaction of KO on SO in %EE of exp 2 (d); interaction of SO on KO in %EE of exp 2 (e).

Considering the aforementioned interactions, it is generally desirable that the liquid lipids present high amounts to have high %EE, as well as PS.

3.3.5 Relative drug loading (R-drug loading)

Fig. 8 (a) shows that BW increased the R-drug loading ($p<0.01$), but KO decreased it ($p<0.0001$). The action of the liquid lipids was more complex. Fig. 8 (a) exhibits CO decreasing the R-drug loading, but CC appears to increase it and the

multilevel analysis shows the opposite. At this point, the evaluation of the interactions was necessary.

Fig. 8 (b) exhibits that when CC is at a high level, CO promotes a discrete increase on the R-drug loading, but when CC is low, CO decreases strongly the R-drug loading. On the other hand, if CO is at low or high level, CC always increases the R-drug loading, and this is accentuated when CO is at the high level (Fig. 8 (c)). This explains why the isolated effect of CC was to increase the R-drug loading. Moreover, the interaction of CC with CO also elucidated why in the model its isolated effect was to increase the R-drug loading (Cf. FMM in Supplementary Material). According to Müller *et al*³⁴, the use of lipids with different molecular structures may assure a high drug loading capacity of the lipid matrix of NLCs, because of the formation of many imperfections in the lipid lattice of them.

Additionally, it is important to mention that BW interacted with SO and with CA, but the size effect of these interactions was not big when compared to the interactions of KO and SO, on the one hand, and with LD, on the other. In Fig. 8 (d), we visualize that when KO is at a high level, LD decreased the R-drug loading but it does not have a strong effect if KO is at a low level. Contrarily, Fig. 8 (e) shows that when LD is at a low level KO has no effect on the R-drug loading, but when LD is at a high level KO acted to decrease it. One possible interpretation is that the high amount of KO promote an interaction of this surfactant with LD, avoiding its incorporation into the lipid matrix, which decreases the drug loading. Nevertheless, to confirm this further experiments should be done. It was reported by Pathak *et al*⁵ that the reduction of solid lipids could influence to augment the drug loading capacity of the formulations. Our results suggest that this happens because not necessarily the less amount of solid lipid, but also the addition of liquid lipids contribute to the formation of oily vesicles in the inner of the nanoparticles, which may have more affinity to the drug and, therefore, to enhance the drug loading.

According to our analysis, to improve drug loading, it is important to maintain high level of CC. If BW was the selected solid lipid, high amounts of it also contributes to reach high drug loading. Moreover, KO acted to decrease drug loading, so its use should occur in moderate levels.

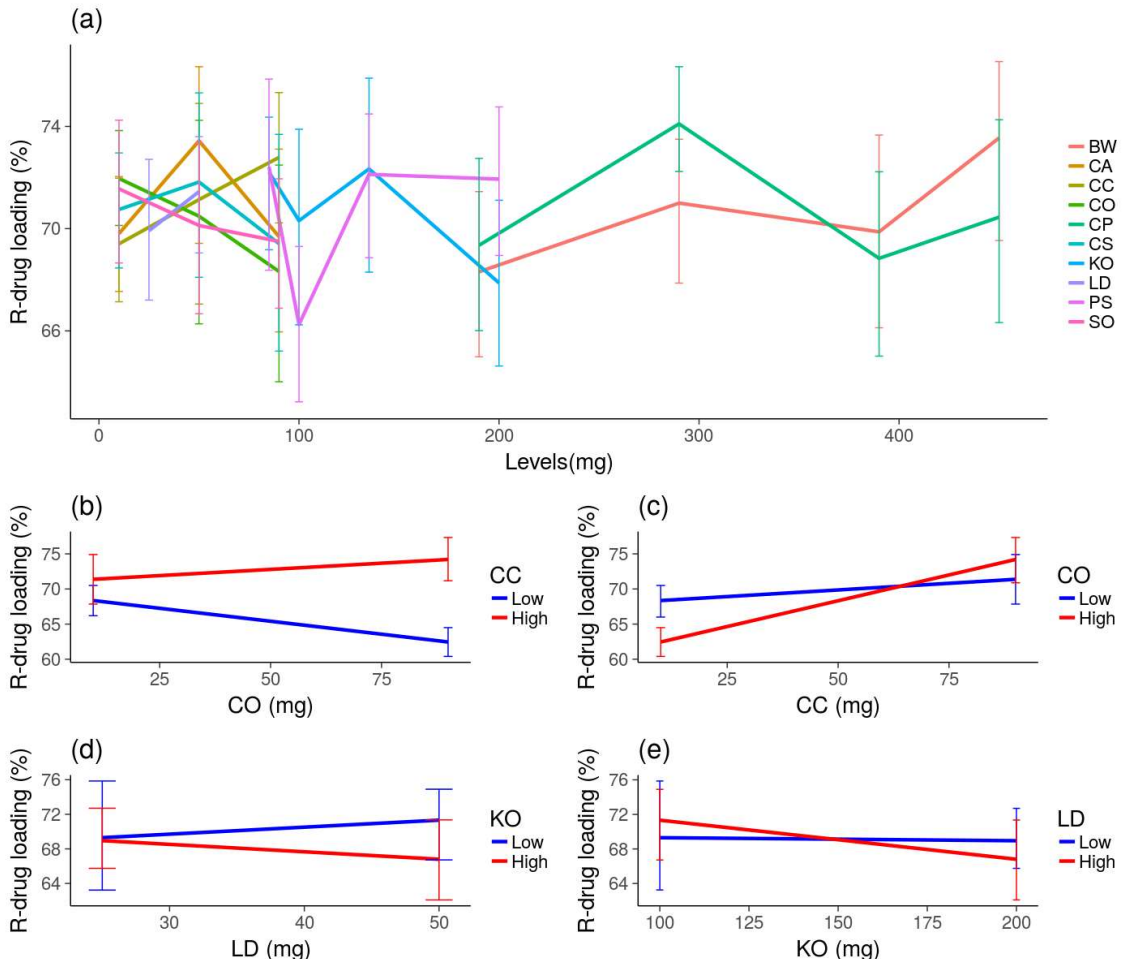


Figure 11. Relative drug loading (%RDL) distribution from exp 1 and 2 at low and high levels of each excipient (BW= beeswax, CA= castor oil, CC= capric/caprylic oil, CO= corn oil, CP= cetyl palmitate, CS= cottonseed oil, KO= poloxamer 188, LD= lidocaine, PS=polysorbate 80, SO= sesame oil). Error bars correspond to the standard deviation of samples mean of each experiment. The values of levels of each experiment are in STables 1 and 2 (a); interaction of CO on CC in %RDL of exp 2 (b); interaction of CC on CO in %RDL of exp 2 (c); interaction of LD on KO in %RDL of exp 2 (d) and interaction of KO on LD in %RDL of exp 2.

3.4 Stability of the optimal formulations

All the formulations were analyzed according to z-average, PDI and zeta potential for 30 days. The formulations that presented the best stability, relative low PDI and higher %EE and %DL were evaluated after 6 months. The selected formulations were: NLC # 3; 6; 7 and 8 from exp 1; and NLC # 6; 7; 15; 16 from exp 2. Interestingly, the majority of the selected formulations presented high levels of CA and BW. CA presents hydroxyl groups in its molecules, which may improve thermodynamic stability ³⁵. Besides, BW and CA seems to have a superior

homogeneity than CA with CP (data not shown). The results from z-average, PDI and zeta potential of days 0, 30 and 180 are on Fig. 9. According to these, NLC # 8_1 did not meet good stability criteria, because it had an increase in z-average and PDI in 180 days. Its PDI was higher than 0,4, which is not a good parameter to monodisperse formulations³⁶.

From exp 1, we repeated the determination of %EE and %DL of NLC# 3, 6 and 7. The formulations NLC #6 and #7 had a pronounced decrease in encapsulated LD, and were excluded to the release profile study, because they profiles could not represent the reality to that respective samples. Therefore, only NLC#3 had its release profile evaluated.

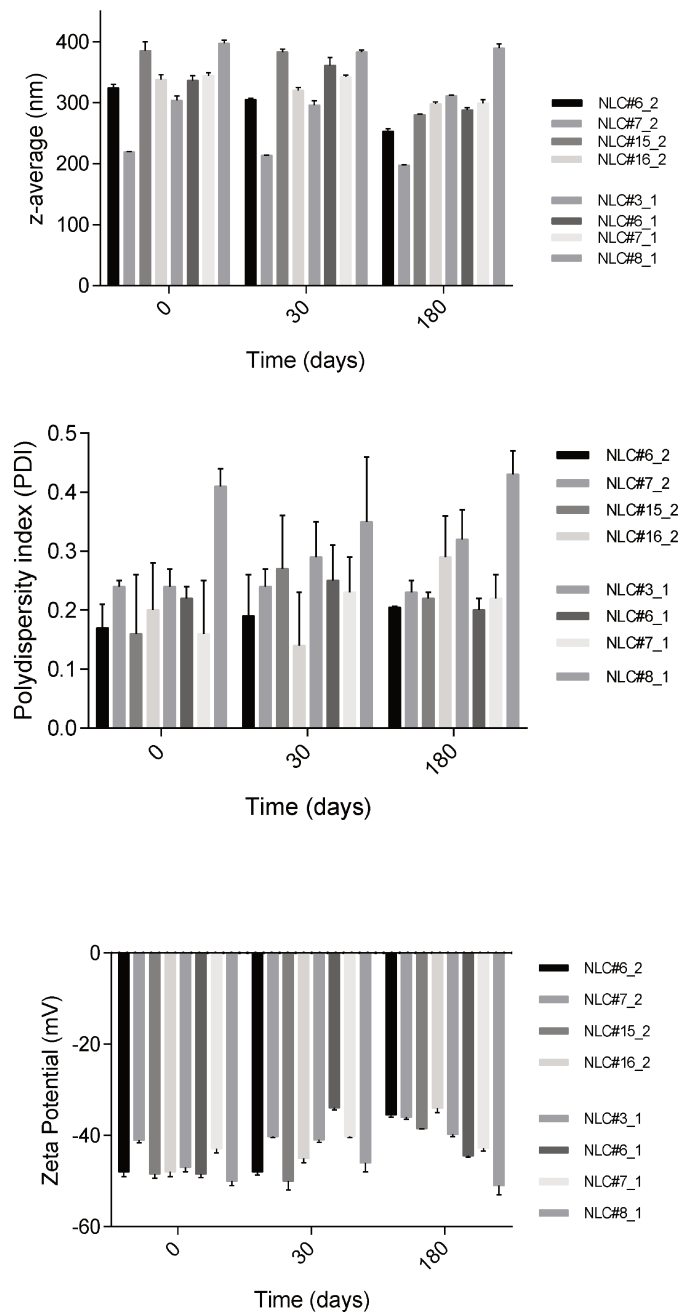


Figure 9. Stability study of optimal NLC formulations (NLC#3_1, NLC#6_1, NLC#7_1 and NLC#8_1 are formulations from experiment 1, and NLC#6_2, NLC#7_2, NLC#15_2 and NLC#16_2 are formulations from experiment 2). Error bars correspond to standard deviation of triplicate data. Z-average (top); PDI (middle) and zeta potential (down), during 6 months of storage.

3.5 LD release profile

Based on the stability studies, the release profile of LD was carried out using the most stable formulation, NLC#3_1, compared to the free drug. The release profile of

LD shown in Fig. 10 confirms that NLC modified LD release; after the first hour, they presented distinct releases, and after 24 hours, free LD was completely released, while only 53% of the encapsulated LD reached the acceptor compartment.

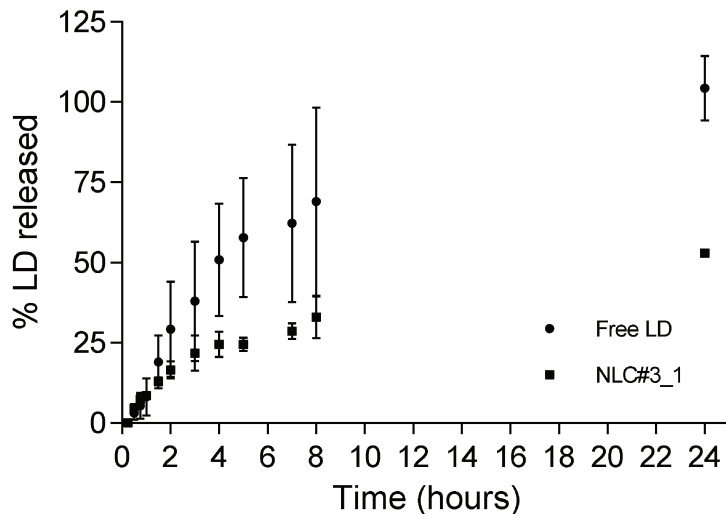


Figure 10. LD release profile (comparison between the free drug and the encapsulated in NLC#3_1). The bar errors are standard deviation and the experiment was carried out in duplicates.

Linear regression analysis was used to fit a model to the data of free-LD sample (FL) and encapsulated sample (ES). The models generated were, respectively, $FL(t) = 19.341t^{0.556}$ and $ES(t) = 10.618t^{0.517}$, where t is the time. The R^2 were 0.9378 for FL, and 0.9736 for ES (details of this model in Supplementary Material). We also applied difference and similarity tests to the profiles: the difference index was 43.3 and the similarity index was 30.4. According to the FDA guideline, it is allowed an empirical 10 % average difference at each sample time point, this would determine a similarity factor of 50³⁷. For this reason, two profiles are considered pharmaceutically equivalent if the similarity index is in the range 50-100 and the difference index is lower than 15³⁸. The results show that the two profiles analyzed are pharmaceutically highly non-equivalent. Actually, since FL had an exponent $n \approx 6$, it presented an anomalous subdiffusion. On the other side, as ES had an exponent $n \approx 5$, its model is actually a Higuchi model and so presented a Fickian diffusion³⁹. This

is an evidence that the NLC studied made the LD release slower in the long term and converted the mean squared displacement of the LD into a linear function of time.

3.6 Transmission electron microscopy

The morphology of NLCs were obtained by TEM images (Fig. 11). The micrographs revealed intact NLCs, with spherical shapes and defined borders, for both samples (with and without LD), indicating that LD-loaded NLC did not presented shape changes because of the drug inclusion. Also, the sizes of the nanoparticles were consistent with those determined by DLS (data not shown).

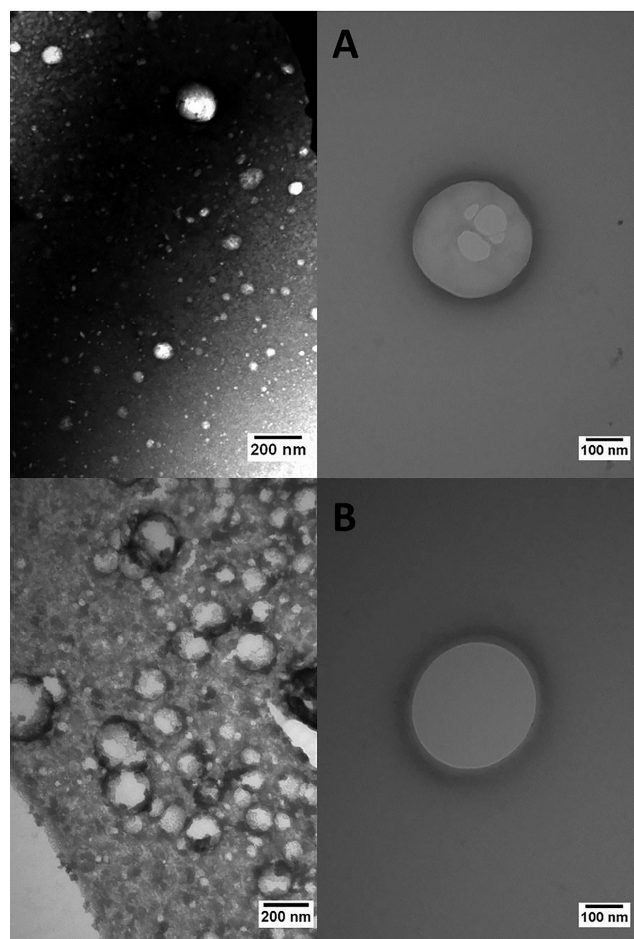


Figure 11. TEM micrographs of NLC#3 empty (A) and LD-loaded NLC#3 (B), both from exp 2. Magnification: 60,000 (left) and 100,000 (right side).

3.7 NLC containing BW, CA, PS and LD

In order to confirm the predicted results presented above, a new NLC was made containing BW, CA, PS and LD. The choice of these excipients relies on the fact that they contributed to decrease PDI and to increase %EE, R-drug loading and zeta potential (in module).

The physicochemical properties of the new NLC were: z-average (267 ± 7) nm, PDI ($0,17 \pm 0,02$), zeta potential (-41 ± 2) mV, %EE ($80,1 \pm 0,1$) % and relative drug loading ($80,1 \pm 0,1$) %, which successfully confirmed the aforementioned results.

4 Conclusions:

As a robust drug delivery system⁸, we believe that the excipient interactions information could help those who want to encapsulate different drugs or active molecules into NLCs. The statistical models were appropriate and elucidated the behavior among the excipients. Our analysis exhibited that CA, CP, CC and PS were the most interactive excipients along the different responses, and we outlined some general patterns in order to make optimal NLCs. Thus, we can predict the best quantities and proportions of the excipients that will reach a desirable feature in NLC, with a method that can also be applied to the other drug delivery systems.

Acknowledgments

The authors have no conflict of interest to declare. The authors would like to acknowledge Coordination for the Improvement of Higher Education Personnel (CAPES), National Council for Scientific and Technological Development (CNPq), São Paulo Research Foundation (FAPESP) Grant number 14/14457-5.

Supplementary material

STable 1: Design of Experiment of experiment 1

STable 2: Design of Experiment of experiment 2

Models to each physicochemical output: GLS, IMM, FMM and linear models

SFigures 1 and 2: statistical assumptions of the models

SFigure 3: release profiles of LD and the fitted models

STable 1. Hall's design of experiment 1 (Factors: CP=cetyl palmitate, BW=beeswax, CC=capric/caprylic oil, SO=sesame oil, KO=poloxamer 188, CS=cottonseed oil, CO=corn oil, CA=castor oil, PS=polysorbate 80, LD=lidocaine. The values on each column refers to the amount of excipient, in milligrams, in each formulation. Formulations: NLC#1_1 refers to the first formulation of experiment 1, and so on to the subsequent formulations).

Factors											
Formulation	1	2	3	4	5	6	7	8	9	10	
	CP	BW	CC	SO	KO	CS	CO	CA	PS	LD	
NLC#1_1	290	290	10	10	85	10	10	10	135	25	
NLC#2_1	450	290	10	10	135	50	50	10	85	50	
NLC#3_1	290	450	10	10	135	50	10	50	85	25	
NLC#4_1	450	450	10	10	85	10	50	50	85	25	
NLC#5_1	290	290	50	10	135	10	50	50	135	50	
NLC#6_1	450	290	50	10	85	50	10	50	135	50	
NLC#7_1	290	450	50	10	85	50	50	10	135	25	
NLC#8_1	450	450	50	10	135	10	10	10	85	50	
NLC#9_1	290	290	10	50	85	50	50	50	85	50	
NLC#10_1	450	290	10	50	135	10	10	50	135	25	
NLC#11_1	290	450	10	50	135	10	50	10	135	50	
NLC#12_1	450	450	10	50	85	50	10	10	135	50	
NLC#13_1	290	290	50	50	135	50	10	10	85	25	
NLC#14_1	450	290	50	50	85	10	50	10	85	25	
NLC#15_1	290	450	50	50	85	10	10	50	85	50	
NLC#16_1	450	450	50	50	135	50	50	50	135	25	

STable 2. Hall's design of experiment 2 (Factors: CP=cetyl palmitate, BW=beeswax, CC=capric/caprylic oil, SO=sesame oil, KO=poloxamer 188, CS=cottonseed oil, CO=corn oil, CA=castor oil, PS=polysorbate 80, LD=lidocaine. The values on each column refers to the amount of excipient, in milligrams, in each formulation. Formulations: NLC#1_2 refers to the first formulation of experiment 2, and so on to the subsequent formulations).

Factors											
Formulation	1	2	3	4	5	6	7	8	9	10	
	CP	BW	CC	SO	KO	CS	CO	CA	PS	LD	
NLC#1_2	190	190	10	10	100	10	10	10	200	25	
NLC#2_2	390	190	10	10	200	90	90	10	100	50	
NLC#3_2	190	390	10	10	200	90	10	90	100	25	
NLC#4_2	390	390	10	10	100	10	90	90	100	25	
NLC#5_2	190	190	90	10	200	10	90	90	200	50	
NLC#6_2	390	190	90	10	100	90	10	90	200	50	
NLC#7_2	190	390	90	10	100	90	90	10	200	25	
NLC#8_2	390	390	90	10	200	10	10	10	100	50	

NLC#9_2	190	190	10	90	100	90	90	90	100	50
NLC#10_2	390	190	10	90	200	10	10	90	200	25
NLC#11_2	190	390	10	90	200	10	90	10	200	50
NLC#12_2	390	390	10	90	100	90	10	10	200	50
NLC#13_2	190	190	90	90	200	90	10	10	100	25
NLC#14_2	390	190	90	90	100	10	90	10	100	25
NLC#15_2	190	390	90	90	100	10	10	90	100	50
NLC#16_2	390	390	90	90	200	90	90	90	200	25

Models to each physicochemical output (z-average, polydispersity index, zeta potential, entrapment efficiency and relative drug loading):

-----Z-AVERAGE-----

GM

Call:

```
lm.default(formula = scale(average) ~ CA + CP + CA:CP + CA:PS,
  data = design)
```

Residuals:

Min	1Q	Median	3Q	Max
-1.45268	-0.45560	0.04302	0.42765	1.13915

Coefficients:

	Estimate	Std. Error	t value	Pr(> t)
(Intercept)	-3.520e+00	6.100e-01	-5.770	3.89e-06 ***
CA	5.509e-02	1.128e-02	4.882	4.18e-05 ***
CP	9.336e-03	1.790e-03	5.216	1.70e-05 ***
CA:CP	-7.521e-05	3.519e-05	-2.137	0.04178 *
CA:PS	-1.486e-04	4.770e-05	-3.115	0.00433 **

Signif. codes: 0 '****' 0.001 '***' 0.01 '**' 0.05 '*' 0.1 ' ' 1

Residual standard error: 0.6256 on 27 degrees of freedom

Multiple R-squared: 0.6592, Adjusted R-squared: 0.6087

F-statistic: 13.05 on 4 and 27 DF, p-value: 4.839e-06

M1

Call:

```
lm.default(formula = scale(average) ~ CA + CP + CA:CP + CA:PS,
  data = design1)
```

Residuals:

Min	1Q	Median	3Q	Max
-1.07554	-0.32038	0.01749	0.30300	0.99751

Coefficients:

	Estimate	Std. Error	t value	Pr(> t)
(Intercept)	-2.4001718	1.5256648	-1.573	0.1440
CA	0.0091684	0.0416788	0.220	0.8299
CP	0.0068238	0.0040345	1.691	0.1189
CA:CP	0.0001040	0.0001212	0.858	0.4092
CA:PS	-0.0004709	0.0002239	-2.103	0.0593 .

Signif. codes: 0 '***' 0.001 '**' 0.01 '*' 0.05 '.' 0.1 ' ' 1

Residual standard error: 0.6991 on 11 degrees of freedom

Multiple R-squared: 0.6416, Adjusted R-squared: 0.5112

F-statistic: 4.922 on 4 and 11 DF, p-value: 0.01604

M2

Call:

```
lm.default(formula = scale(average) ~ CA + CP + CA:CP + CA:PS,
  data = design2)
```

Residuals:

Min	1Q	Median	3Q	Max
-0.52687	-0.35604	-0.00559	0.22379	0.71864

Coefficients:

	Estimate	Std. Error	t value	Pr(> t)
(Intercept)	-2.926e+00	5.575e-01	-5.248	0.000273 ***
CA	5.223e-02	8.976e-03	5.818	0.000116 ***
CP	7.982e-03	1.819e-03	4.388	0.001085 **
CA:CP	-4.626e-05	3.092e-05	-1.496	0.162692
CA:PS	-1.772e-04	4.066e-05	-4.359	0.001138 **

Signif. codes: 0 '***' 0.001 '**' 0.01 '*' 0.05 '.' 0.1 ' ' 1

Residual standard error: 0.4509 on 11 degrees of freedom

Multiple R-squared: 0.8509, Adjusted R-squared: 0.7967

F-statistic: 15.69 on 4 and 11 DF, p-value: 0.0001617

GLS

Generalized least squares fit by maximum likelihood

Model: scale(average) ~ 1

Data: design

AIC	BIC	logLik
93.79611	96.72758	-44.89805

Coefficients:

	Value	Std.Error	t-value	p-value
(Intercept)	0	0.1767767	0	1

Standardized residuals:

Min	Q1	Med	Q3	Max
-2.2185950	-0.6182530	0.1765478	0.6545023	1.6909655

Residual standard error: 0.984251

Degrees of freedom: 32 total; 31 residual

IMM

Linear mixed-effects model fit by maximum likelihood

Data: design

AIC	BIC	logLik
200.9757	205.3729	-97.48785

Random effects:

Formula: ~1 | experiment

(Intercept) Residual

StdDev: 1.035557 5.009187

Fixed effects: entrapment ~ 1

Value	Std.Error	DF	t-value	p-value
(Intercept)	72.10625	1.167434	30	61.76471 0

Standardized Within-Group Residuals:

Min	Q1	Med	Q3	Max
-2.7442226	-0.2917065	0.2562941	0.6645139	1.3243316

Number of Observations: 32

Number of Groups: 2

ANOVA

Model	df	AIC	BIC	logLik	Test	L.Ratio	p-value
GLS	1	2	93.79611	96.72758	-44.89805		
IMM	2	3	95.79611	100.19332	-44.89805	1 vs 2	1.079874e-08 0.9999

FMM

Linear mixed-effects model fit by maximum likelihood

Data: design

AIC	BIC	logLik
69.35171	79.61187	-27.67586

Random effects:

Formula: ~1 | experiment
 (Intercept) Residual
 StdDev: 1.487302e-05 0.5746075

Fixed effects: scale(average) ~ CA + CP + CA:CP + CA:PS

	Value	Std.Error	DF	t-value	p-value
(Intercept)	-3.519776	0.6100451	26	-5.769698	0.0000
CA	0.055092	0.0112846	26	4.882085	0.0000
CP	0.009336	0.0017899	26	5.216234	0.0000
CA:CP	-0.000075	0.0000352	26	-2.137326	0.0421
CA:PS	-0.000149	0.0000477	26	-3.114799	0.0044

Correlation:

	(Intr)	CA	CP	CA:CP
CA	-0.693			
CP	-0.957	0.654		
CA:CP	0.706	-0.747	-0.772	
CA:PS	-0.117	-0.305	0.177	-0.340

Standardized Within-Group Residuals:

Min	Q1	Med	Q3	Max
-2.52813191	-0.79288732	0.07486548	0.74425088	1.98248726

Number of Observations: 32

Number of Groups: 2

ANOVA

Model	df	AIC	BIC	logLik	Test	L.Ratio	p-value
IMM	1	3	95.79611	100.19332	-44.89805		
FMM	2	7	69.35171	79.61187	-27.67586	1 vs 2	34.44439 <.0001

-----POLYDISPERSITY INDEX-----

GM

Call:

```
lm.default(formula = scale(l(log(dispersity))) ~ PS + BW + CA +
  CP:BW + CP:PS + CA:CP + CA:CO, data = design)
```

Residuals:

Min	1Q	Median	3Q	Max
-1.45023	-0.37137	0.00196	0.37135	1.26991

Coefficients:

	Estimate	Std. Error	t value	Pr(> t)
(Intercept)	-6.493e-01	6.099e-01	-1.064	0.297711
PS	3.571e-02	7.662e-03	4.660	9.85e-05 ***
BW	-8.720e-03	3.352e-03	-2.601	0.015658 *
CA	-3.459e-02	1.213e-02	-2.852	0.008792 **
BW:CP	3.665e-05	9.520e-06	3.850	0.000769 ***
PS:CP	-1.237e-04	2.429e-05	-5.094	3.28e-05 ***
CA:CP	1.307e-04	3.699e-05	3.532	0.001700 **
CA:CO	-1.445e-04	7.129e-05	-2.027	0.053918 .

Signif. codes:	0 ****	0.001 ***	0.01 **	0.05 *
	0.1 '	0.1 ''	1	

Residual standard error: 0.6411 on 24 degrees of freedom
 Multiple R-squared: 0.6818, Adjusted R-squared: 0.589
 F-statistic: 7.346 on 7 and 24 DF, p-value: 9.518e-05

M1

Call:

```
lm.default(formula = scale(l(log(dispersity))) ~ PS + BW + CA +
  CP:BW + CP:PS + CA:CP + CA:CO, data = design1)
```

Residuals:

Min	1Q	Median	3Q	Max
-1.81233	-0.32224	0.04695	0.46209	0.77054

Coefficients:

	Estimate	Std. Error	t value	Pr(> t)
(Intercept)	-7.874e-01	1.538e+00	-0.512	0.623
PS	3.644e-02	4.715e-02	0.773	0.462
BW	-7.311e-03	1.415e-02	-0.517	0.619
CA	-5.488e-02	5.929e-02	-0.926	0.382
BW:CP	3.281e-05	3.753e-05	0.874	0.408
PS:CP	-1.370e-04	1.268e-04	-1.080	0.312
CA:CP	1.806e-04	1.522e-04	1.187	0.269
CA:CO	2.318e-04	4.435e-04	0.523	0.615

Residual standard error: 0.8693 on 8 degrees of freedom
 Multiple R-squared: 0.5969, Adjusted R-squared: 0.2442
 F-statistic: 1.692 on 7 and 8 DF, p-value: 0.2382

M2

Call:

```
lm.default(formula = scale(l(log(dispersity))) ~ PS + BW + CA +
```

CP:BW + CP:PS + CA:CP + CA:CO, data = design2)

Residuals:

	Min	1Q	Median	3Q	Max
	-0.81007	-0.37348	-0.02647	0.41920	0.52431

Coefficients:

	Estimate	Std. Error	t value	Pr(> t)
(Intercept)	-8.993e-01	7.012e-01	-1.282	0.23561
PS	3.824e-02	1.041e-02	3.673	0.00628 **
BW	-8.904e-03	5.428e-03	-1.640	0.13956
CA	-2.706e-02	1.354e-02	-1.998	0.08072 .
BW:CP	3.395e-05	1.802e-05	1.884	0.09628 .
PS:CP	-1.134e-04	3.511e-05	-3.230	0.01205 *
CA:CP	1.011e-04	4.050e-05	2.497	0.03712 *
CA:CO	-1.162e-04	8.968e-05	-1.296	0.23113

Signif. codes:	0 ****	0.001 ***	0.01 **	0.05 *.
	0.1 '	1		

Residual standard error: 0.5877 on 8 degrees of freedom

Multiple R-squared: 0.8158, Adjusted R-squared: 0.6546

F-statistic: 5.061 on 7 and 8 DF, p-value: 0.01818

GLS

Generalized least squares fit by maximum likelihood

Model: scale(l(log(dispersity))) ~ 1

Data: design

AIC	BIC	logLik
93.79611	96.72758	-44.89805

Coefficients:

	Value	Std.Error	t-value	p-value
(Intercept)	-1.300233e-16	0.1767767	-7.355228e-16	1

Standardized residuals:

Min	Q1	Med	Q3	Max
-2.19955135	-0.79905848	0.07712873	0.50448719	2.00259582

Residual standard error: 0.984251

Degrees of freedom: 32 total; 31 residual

IMM

Linear mixed-effects model fit by maximum likelihood

Data: design

AIC	BIC	logLik
200.9757	205.3729	-97.48785

Random effects:

Formula: ~1 | experiment
 (Intercept) Residual
 StdDev: 1.035557 5.009187

Fixed effects: entrapment ~ 1

Value	Std.Error	DF	t-value	p-value
(Intercept)	72.10625	1.167434	30	61.76471 0

Standardized Within-Group Residuals:

Min	Q1	Med	Q3	Max
-2.7442226	-0.2917065	0.2562941	0.6645139	1.3243316

Number of Observations: 32

Number of Groups: 2

ANOVA

Model	df	AIC	BIC	logLik	Test	L.Ratio	p-value
GLS	1	2	93.79611	96.72758	-44.89805		
IMM	2	3	89.56342	93.96063	-41.78171	1 vs 2	6.232689 0.0125

FMM

Linear mixed-effects model fit by maximum likelihood

Data: design

AIC	BIC	logLik
67.2922	81.94956	-23.6461

Random effects:

Formula: ~1 | experiment
 (Intercept) Residual
 StdDev: 0.3916333 0.4685504

Fixed effects: scale(I(log(dispersity))) ~ PS + BW + CA + CP:BW +
 CP:PS + CA:CP + CA:CO

Value	Std.Error	DF	t-value	p-value
(Intercept)	-0.7655242	0.6071253	23	-1.260900 0.2200
PS	0.0366345	0.0064729	23	5.659697 0.0000
BW	-0.0082606	0.0028328	23	-2.916098 0.0078
CA	-0.0311462	0.0102933	23	-3.025870 0.0060
BW:CP	0.0000321	0.0000082	23	3.937021 0.0007

PS:CP -0.0001169 0.0000206 23 -5.668705 0.0000
 CA:CP 0.0001194 0.0000314 23 3.799857 0.0009
 CA:CO -0.0001093 0.0000612 23 -1.785277 0.0874

Correlation:

	(Intr)	PS	BW	CA	BW:CP	PS:CP	CA:CP
PS	-0.218						
BW		-0.122	-0.761				
CA			-0.288	0.109	-0.338		
BW:CP				-0.100	0.823	-0.929	0.367
PS:CP					-0.018	-0.913	0.759
CA:CP						0.235	0.151
CA:CO							0.049

Standardized Within-Group Residuals:

	Min	Q1	Med	Q3	Max
	-2.67780161	-0.62635129	0.05546289	0.64065629	1.94665901

Number of Observations: 32

Number of Groups: 2

ANOVA

Model	df	AIC	BIC	logLik	Test	L.Ratio	p-value
IMM	1	389.56342	93.96063	-41.78171			
FMM	2	1067.29220	81.94956	-23.64610	1 vs 2	36.27122	<.0001

ZETA POTENTIAL

GM

Call:

```
lm.default(formula = scale(-abs(potential)^3) ~ CA + PS + CS +
  KO:CA + CS:PS + LD:PS + CC:PS, data = design)
```

Residuals:

Min	1Q	Median	3Q	Max
-0.9160	-0.3524	-0.1659	0.2150	1.2809

Coefficients:

	Estimate	Std. Error	t value	Pr(> t)
(Intercept)	-2.146e+00	6.961e-01	-3.083	0.005095 **
CA	2.683e-02	8.798e-03	3.050	0.005508 **
PS	3.131e-02	5.891e-03	5.315	1.88e-05 ***
CS	2.853e-02	1.279e-02	2.231	0.035320 *
CA:KO	-2.621e-04	5.745e-05	-4.562	0.000127 ***
PS:CS	-2.574e-04	8.986e-05	-2.865	0.008540 **
PS:LD	-3.559e-04	7.010e-05	-5.077	3.42e-05 ***

PS:CC 7.426e-05 2.812e-05 2.640 0.014327 *

Signif. codes: 0 '****' 0.001 '**' 0.01 '*' 0.05 '.' 0.1 '' 1

Residual standard error: 0.6476 on 24 degrees of freedom

Multiple R-squared: 0.6753, Adjusted R-squared: 0.5806

F-statistic: 7.132 on 7 and 24 DF, p-value: 0.0001186

M1

Call:

```
lm.default(formula = scale(-abs(potential)^3) ~ CA + PS + CS +
  KO:CA + CS:PS + LD:PS + CC:PS, data = design1)
```

Residuals:

Min	1Q	Median	3Q	Max
-1.27478	-0.31115	0.00257	0.29517	1.47703

Coefficients:

	Estimate	Std. Error	t value	Pr(> t)
(Intercept)	0.1775776	2.2202012	0.080	0.9382
CA	-0.0095410	0.0331653	-0.288	0.7809
PS	0.0114932	0.0205010	0.561	0.5904
CS	-0.0804869	0.0610752	-1.318	0.2240
CA:KO	0.0001349	0.0002900	0.465	0.6542
PS:CS	0.0007229	0.0005541	1.304	0.2283
PS:LD	-0.0003349	0.0001544	-2.169	0.0619 .
PS:CC	-0.0000576	0.0001110	-0.519	0.6178

Signif. codes: 0 '****' 0.001 '**' 0.01 '*' 0.05 '.' 0.1 '' 1

Residual standard error: 0.8239 on 8 degrees of freedom

Multiple R-squared: 0.6379, Adjusted R-squared: 0.3211

F-statistic: 2.014 on 7 and 8 DF, p-value: 0.1737

M2

Call:

```
lm.default(formula = scale(-abs(potential)^3) ~ CA + PS + CS +
  KO:CA + CS:PS + LD:PS + CC:PS, data = design2)
```

Residuals:

Min	1Q	Median	3Q	Max
-0.51541	-0.22858	-0.04658	0.16620	0.70484

Coefficients:

	Estimate	Std. Error	t value	Pr(> t)
(Intercept)	-2.149e+00	7.263e-01	-2.959	0.018169 *
CA	2.425e-02	7.130e-03	3.401	0.009351 **
PS	2.884e-02	5.293e-03	5.449	0.000609 ***
CS	3.352e-02	1.113e-02	3.012	0.016762 *
CA:KO	-2.423e-04	4.455e-05	-5.439	0.000617 ***
PS:CS	-2.775e-04	7.368e-05	-3.766	0.005497 **
PS:LD	-3.175e-04	6.049e-05	-5.249	0.000775 ***
PS:CC	8.249e-05	2.155e-05	3.828	0.005035 **

Signif. codes: 0 '***' 0.001 '**' 0.01 '*' 0.05 '.' 0.1 ' ' 1

Residual standard error: 0.4474 on 8 degrees of freedom

Multiple R-squared: 0.8933, Adjusted R-squared: 0.7999

F-statistic: 9.564 on 7 and 8 DF, p-value: 0.002438

GLS

Generalized least squares fit by maximum likelihood

Model: scale(-abs(potential)^3) ~ 1

Data: design

AIC	BIC	logLik
93.79611	96.72758	-44.89805

Coefficients:

	Value	Std.Error	t-value	p-value
(Intercept)	3.925231e-17	0.1767767	2.220446e-16	1

Standardized residuals:

Min	Q1	Med	Q3	Max
-2.1408953	-0.6158747	-0.3455728	0.8183467	2.2622049

Residual standard error: 0.984251

Degrees of freedom: 32 total; 31 residual

IMM

Linear mixed-effects model fit by maximum likelihood

Data: design

AIC	BIC	logLik
200.9757	205.3729	-97.48785

Random effects:

Formula: ~1 | experiment

(Intercept) Residual
 StdDev: 1.035557 5.009187

Fixed effects: entrapment ~ 1
 Value Std.Error DF t-value p-value
 (Intercept) 72.10625 1.167434 30 61.76471 0

Standardized Within-Group Residuals:
 Min Q1 Med Q3 Max
 -2.7442226 -0.2917065 0.2562941 0.6645139 1.3243316

Number of Observations: 32

Number of Groups: 2

ANOVA

Model	df	AIC	BIC	logLik	Test	L.Ratio	p-value
GLS	1	2	93.79611	96.72758	-44.89805		
IMM	2	3	95.79611	100.19332	-44.89805	1 vs 2	1.021272e-08 0.9999

FMM

Linear mixed-effects model fit by maximum likelihood

Data: design

AIC	BIC	logLik
73.79691	88.45427	-26.89845

Random effects:

Formula: ~1 | experiment

(Intercept) Residual

StdDev: 1.149737e-05 0.5608163

Fixed effects: scale(-abs(potential)^3) ~ CA + PS + CS + KO:CA +
 CS:PS + LD:PS + CC:PS

	Value	Std.Error	DF	t-value	p-value
(Intercept)	-2.1457707	0.6960688	23	-3.082699	0.0053
CA	0.0268340	0.0087978	23	3.050078	0.0057
PS	0.0313135	0.0058915	23	5.315041	0.0000
CS	0.0285265	0.0127891	23	2.230540	0.0358
CA:KO	-0.0002621	0.0000575	23	-4.561868	0.0001
PS:CS	-0.0002574	0.0000899	23	-2.864615	0.0088
PS:LD	-0.0003559	0.0000701	23	-5.077218	0.0000
PS:CC	0.0000743	0.0000281	23	2.640474	0.0146

Correlation:

(Intr)	CA	PS	CS	CA:KO	PS:CS	PS:LD
CA	-0.537					
PS	-0.849	0.494				

CS	-0.809	0.343	0.666				
CA:KO	0.559	-0.913	-0.576	-0.430			
PS:CS	0.798	-0.355	-0.696	-0.961	0.441		
PS:LD	0.173	-0.282	-0.581	-0.133	0.308	0.136	
PS:CC	-0.292	0.130	0.164	0.431	-0.241	-0.496	-0.074

Standardized Within-Group Residuals:

Min	Q1	Med	Q3	Max
-1.6332653	-0.6284654	-0.2958900	0.3832948	2.2840192

Number of Observations: 32

Number of Groups: 2

ANOVA

Model	df	AIC	BIC	logLik	Test	L.Ratio	p-value
IMM	1	3	95.79611	100.19332	-44.89805		
FMM	2	10	73.79691	88.45427	-26.89845	1 vs 2	35.9992 <.0001

-----ENTRAPMENT EFFICIENCY-----

GM

Call:

```
lm.default(formula = scale(entrapment^10) ~ CC + PS + SO + CS +
  CC:CS + SO:KO + CC:PS + CO:PS + PS:KO, data = design)
```

Residuals:

Min	1Q	Median	3Q	Max
-1.58705	-0.35245	0.06279	0.41332	1.23768

Coefficients:

	Estimate	Std. Error	t value	Pr(> t)
(Intercept)	3.956e-01	8.899e-01	0.445	0.661008
CC	-4.729e-02	1.921e-02	-2.461	0.022160 *
PS	1.900e-02	9.493e-03	2.001	0.054833 .
SO	-1.022e-01	3.689e-02	-2.772	0.011124 *
CS	3.752e-02	1.262e-02	2.973	0.007025 **
CC:CS	-1.347e-03	3.920e-04	-3.436	0.002360 **
SO:KO	9.359e-04	3.048e-04	3.071	0.005597 **
CC:PS	8.662e-04	2.150e-04	4.028	0.000563 ***
PS:CO	-1.113e-04	3.583e-05	-3.106	0.005157 **
PS:KO	-3.021e-04	1.017e-04	-2.970	0.007064 **

Signif. codes: 0 '****' 0.001 '***' 0.01 '**' 0.05 '*' 0.1 '.' 1 ''

Residual standard error: 0.7395 on 22 degrees of freedom
 Multiple R-squared: 0.6119, Adjusted R-squared: 0.4532
 F-statistic: 3.854 on 9 and 22 DF, p-value: 0.0047

M1

Call:

```
lm.default(formula = scale(entrainment^10) ~ CC + PS + SO + CS +
  CC:CS + SO:KO + CC:PS + CO:PS + PS:KO, data = design1)
```

Residuals:

	Min	1Q	Median	3Q	Max
	-1.05408	-0.34491	-0.06826	0.40301	1.26035

Coefficients: (1 not defined because of singularities)

	Estimate	Std. Error	t value	Pr(> t)
(Intercept)	-0.1514001	3.1136549	-0.049	0.963
CC	0.0322723	0.0925544	0.349	0.738
PS	0.0180448	0.0244654	0.738	0.485
SO	-0.0171733	0.0336521	-0.510	0.626
CS	-0.0033979	0.0253941	-0.134	0.897
CC:CS	0.0006364	0.0007061	0.901	0.397
SO:KO	-0.0001749	0.0002850	-0.614	0.559
CC:PS	-0.0005624	0.0008343	-0.674	0.522
PS:CO	-0.0000982	0.0001324	-0.742	0.482
PS:KO	NA	NA	NA	NA

Residual standard error: 0.8447 on 7 degrees of freedom
 Multiple R-squared: 0.667, Adjusted R-squared: 0.2864
 F-statistic: 1.753 on 8 and 7 DF, p-value: 0.237

M2

Call:

```
lm.default(formula = scale(entrainment^10) ~ CC + PS + SO + CS +
  CC:CS + SO:KO + CC:PS + CO:PS + PS:KO, data = design2)
```

Residuals:

	Min	1Q	Median	3Q	Max
	-0.55121	-0.33946	0.06841	0.20246	0.65734

Coefficients: (1 not defined because of singularities)

	Estimate	Std. Error	t value	Pr(> t)
(Intercept)	-3.931e-01	1.156e+00	-0.340	0.7437

CC	-3.176e-02	1.946e-02	-1.632	0.1467
PS	-4.150e-03	6.298e-03	-0.659	0.5310
SO	1.883e-02	8.889e-03	2.118	0.0719 .
CS	1.015e-03	7.206e-03	0.141	0.8919
CC:CS	-2.014e-04	1.166e-04	-1.727	0.1278
SO:KO	-1.275e-05	5.402e-05	-0.236	0.8202
CC:PS	3.863e-04	1.285e-04	3.008	0.0197 *
PS:CO	-9.160e-05	2.947e-05	-3.108	0.0171 *
PS:KO	NA	NA	NA	NA

Signif. codes: 0 '****' 0.001 '**' 0.01 '*' 0.05 '.' 0.1 '' 1

Residual standard error: 0.5272 on 7 degrees of freedom
 Multiple R-squared: 0.8703, Adjusted R-squared: 0.7221
 F-statistic: 5.872 on 8 and 7 DF, p-value: 0.01534

GLS

Generalized least squares fit by maximum likelihood

Model: scale(entrainment^10) ~ 1

Data: design

AIC BIC logLik

93.79611 96.72758 -44.89805

Coefficients:

	Value	Std.Error	t-value	p-value	
(Intercept)	-3.925231e-17	0.1767767	-2.220446e-16	1	

Standardized residuals:

Min	Q1	Med	Q3	Max
-1.713369186	-0.562866660	-0.001876848	0.464746499	2.240842593

Residual standard error: 0.984251

Degrees of freedom: 32 total; 31 residual

IMM

Linear mixed-effects model fit by maximum likelihood

Data: design

AIC BIC logLik

95.44195 99.83916 -44.72097

Random effects:

Formula: ~1 | experiment

(Intercept) Residual

StdDev: 0.2095552 0.9616843

Fixed effects: scale(entrainment^10) ~ 1

	Value	Std.Error	DF	t-value	p-value
(Intercept)	-1.301747e-16	0.2291253	30	-5.681377e-16	1

Standardized Within-Group Residuals:

Min	Q1	Med	Q3	Max
-1.610398718	-0.617390254	0.002418779	0.532407308	2.150249733

Number of Observations: 32

Number of Groups: 2

ANOVA

Model	df	AIC	BIC	logLik	Test	L.Ratio	p-value
GLS	1	2	93.79611	96.72758	-44.89805		
IMM	2	3	95.44195	99.83916	-44.72097	1 vs 2	0.3541579 0.5518

FMM

Linear mixed-effects model fit by maximum likelihood

Data: design

AIC	BIC	logLik
83.45179	101.0406	-29.72589

Random effects:

Formula: ~1 | experiment

(Intercept) Residual

StdDev: 0.1476047 0.5997892

Fixed effects: scale(entrainment^10) ~ CC + PS + SO + CS + CC:CS + SO:KO + CC:PS + CO:PS + PS:KO

	Value	Std.Error	DF	t-value	p-value
(Intercept)	0.7402666	0.9452168	21	0.783171	0.4423
CC	-0.0518870	0.0193540	21	-2.680944	0.0140
PS	0.0186971	0.0092907	21	2.012456	0.0542
SO	-0.1065085	0.0363361	21	-2.931202	0.0080
CS	0.0370397	0.0123567	21	2.997543	0.0069
CC:CS	-0.0013752	0.0003845	21	-3.576915	0.0018
SO:KO	0.0009716	0.0003003	21	3.235319	0.0040
CC:PS	0.0009050	0.0002139	21	4.230599	0.0004
PS:CO	-0.0001159	0.0000354	21	-3.278344	0.0036
PS:KO	-0.0003171	0.0001006	21	-3.151654	0.0048

Correlation:

(Intr)	CC	PS	SO	CS	CC:CS	SO:KO	CC:PS	PS:CO
--------	----	----	----	----	-------	-------	-------	-------

CC -0.839
 PS -0.372 0.235
 SO -0.239 0.270 -0.731
 CS -0.055 -0.079 0.704 -0.849
 CC:CS -0.196 0.317 -0.681 0.937 -0.916
 SO:KO 0.287 -0.350 0.700 -0.990 0.842 -0.951
 CC:PS 0.650 -0.816 0.242 -0.725 0.585 -0.792 0.786
 PS:CO -0.400 0.527 0.133 0.126 -0.090 0.204 -0.173 -0.486
 PS:KO -0.258 0.336 -0.757 0.960 -0.818 0.930 -0.975 -0.764 0.108

Standardized Within-Group Residuals:

Min	Q1	Med	Q3	Max
-2.41108215	-0.67560455	0.04708529	0.70748546	2.05053814

Number of Observations: 32

Number of Groups: 2

ANOVA

Model	df	AIC	BIC	logLik	Test	L.Ratio	p-value
IMM	1	3	95.44195	99.83916	-44.72097		
FMM	2	12	83.45179	101.04062	-29.72589	1 vs 2	29.99016 4e-04

-----RELATIVE DRUG LOADING-----

GM

Call:

```
lm.default(formula = scale/loading) ~ CC + CO + KO + BW + CO:CC +
  KO:LD + KO:SO + BW:SO + BW:CA, data = design)
```

Residuals:

Min	1Q	Median	3Q	Max
-1.0606	-0.4171	-0.1091	0.4611	1.1111

Coefficients:

	Estimate	Std. Error	t value	Pr(> t)
(Intercept)	9.311e-01	6.431e-01	1.448	0.161751
CC	-1.499e-02	6.122e-03	-2.448	0.022811 *
CO	-3.652e-02	6.545e-03	-5.580	1.31e-05 ***
KO	-3.344e-02	6.981e-03	-4.790	8.77e-05 ***
BW	6.000e-03	1.606e-03	3.735	0.001148 **
CC:CO	5.668e-04	1.113e-04	5.090	4.24e-05 ***
KO:LD	4.720e-04	1.056e-04	4.468	0.000193 ***
KO:SO	2.496e-04	6.864e-05	3.637	0.001457 **
BW:SO	-1.121e-04	2.994e-05	-3.744	0.001124 **

BW:CA 2.487e-05 1.187e-05 2.096 0.047785 *

Signif. codes: 0 '****' 0.001 '**' 0.01 '*' 0.05 '.' 0.1 '' 1

Residual standard error: 0.637 on 22 degrees of freedom

Multiple R-squared: 0.712, Adjusted R-squared: 0.5942

F-statistic: 6.044 on 9 and 22 DF, p-value: 0.0002797

M1

Call:

lm.default(formula = scale(loadings) ~ CC + CO + KO + BW + CO:CC +
KO:LD + KO:SO + BW:SO + BW:CA, data = design1)

Residuals:

Min	1Q	Median	3Q	Max
-0.91228	-0.36385	-0.04845	0.34305	0.70087

Coefficients:

	Estimate	Std. Error	t value	Pr(> t)
(Intercept)	4.352e-01	1.431e+00	0.304	0.7714
CC	-3.227e-02	2.231e-02	-1.446	0.1982
CO	-4.426e-02	2.382e-02	-1.858	0.1125
KO	-5.337e-02	2.544e-02	-2.098	0.0807 .
BW	1.139e-02	4.674e-03	2.436	0.0507 .
CC:CO	6.967e-04	6.752e-04	1.032	0.3420
KO:LD	7.033e-04	2.835e-04	2.481	0.0478 *
KO:SO	9.165e-04	4.917e-04	1.864	0.1116
BW:SO	-3.191e-04	1.416e-04	-2.254	0.0651 .
BW:CA	4.576e-05	2.710e-05	1.688	0.1423

Signif. codes: 0 '****' 0.001 '**' 0.01 '*' 0.05 '.' 0.1 '' 1

Residual standard error: 0.7479 on 6 degrees of freedom

Multiple R-squared: 0.7762, Adjusted R-squared: 0.4406

F-statistic: 2.313 on 9 and 6 DF, p-value: 0.1598

M2

Call:

lm.default(formula = scale(loadings) ~ CC + CO + KO + BW + CO:CC +
KO:LD + KO:SO + BW:SO + BW:CA, data = design2)

Residuals:

Min	1Q	Median	3Q	Max
-0.66861	-0.12715	-0.00142	0.14162	0.58996

Coefficients:

	Estimate	Std. Error	t value	Pr(> t)
(Intercept)	8.692e-01	7.001e-01	1.242	0.26074
CC	-5.894e-03	6.906e-03	-0.853	0.42618
CO	-2.935e-02	7.748e-03	-3.788	0.00909 **
KO	-2.592e-02	1.016e-02	-2.552	0.04339 *
BW	3.776e-03	2.300e-03	1.642	0.15173
CC:CO	4.604e-04	1.217e-04	3.782	0.00916 **
KO:LD	3.543e-04	1.543e-04	2.297	0.06139 .
KO:SO	1.624e-04	8.837e-05	1.837	0.11581
BW:SO	-6.403e-05	4.232e-05	-1.513	0.18101
BW:CA	1.749e-05	1.305e-05	1.341	0.22852
<hr/>				

Signif. codes: 0 '***' 0.001 '**' 0.01 '*' 0.05 '.' 0.1 ' ' 1

Residual standard error: 0.5219 on 6 degrees of freedom

Multiple R-squared: 0.891, Adjusted R-squared: 0.7276

F-statistic: 5.451 on 9 and 6 DF, p-value: 0.0258

GLS

Generalized least squares fit by maximum likelihood

Model: scale(loadings) ~ 1

Data: design

AIC	BIC	logLik
93.79611	96.72758	-44.89805

Coefficients:

	Value	Std.Error	t-value	p-value
(Intercept)	-5.010803e-16	0.1767767	-2.834538e-15	1

Standardized residuals:

Min	Q1	Med	Q3	Max
-2.0610034	-0.6266444	0.2585870	0.7461744	1.7828892

Residual standard error: 0.984251

Degrees of freedom: 32 total; 31 residual

IMM

Linear mixed-effects model fit by maximum likelihood

Data: design

AIC	BIC	logLik
95.62446	100.0217	-44.81223

Random effects:

Formula: ~1 | experiment

(Intercept) Residual

StdDev: 0.1707542 0.9693261

Fixed effects: scale/loading) ~ 1

	Value	Std.Error	DF	t-value	p-value	
(Intercept)	-5.522072e-16	0.2129747	30	-2.59283e-15	1	

Standardized Within-Group Residuals:

Min	Q1	Med	Q3	Max
-1.9912703	-0.6437657	0.2625685	0.7138775	1.7088740

Number of Observations: 32

Number of Groups: 2

ANOVA

Model	df	AIC	BIC	logLik	Test	L.Ratio	p-value
GLS	1	2	93.79611	96.72758	-44.89805		
IMM	2	3	95.62446	100.02167	-44.81223	1 vs 2	0.1716489 0.6787

FMM

Linear mixed-effects model fit by maximum likelihood

Data: design

AIC	BIC	logLik
73.95932	91.54815	-24.97966

Random effects:

Formula: ~1 | experiment

(Intercept) Residual

StdDev: 1.012721e-05 0.5281768

Fixed effects: scale/loading) ~ CC + CO + KO + BW + CO:CC + KO:LD + KO:SO + BW:SO + BW:CA

	Value	Std.Error	DF	t-value	p-value
(Intercept)	0.9311318	0.6430970	21	1.447887	0.1624
CC	-0.0149855	0.0061218	21	-2.447903	0.0232
CO	-0.0365177	0.0065447	21	-5.579722	0.0000
KO	-0.0334385	0.0069811	21	-4.789899	0.0001
BW	0.0060000	0.0016064	21	3.735059	0.0012
CC:CO	0.0005668	0.0001114	21	5.090215	0.0000
KO:LD	0.0004720	0.0001056	21	4.467605	0.0002

KO:SO	0.0002496	0.0000686	21	3.636520	0.0015
BW:SO	-0.0001121	0.0000299	21	-3.743811	0.0012
BW:CA	0.0000249	0.0000119	21	2.096204	0.0484

Correlation:

(Intr)	CC	CO	KO	BW	CC:CO	KO:LD	KO:SO	BW:SO	
CC	-0.422								
CO	-0.427	0.677							
KO	-0.439	0.370	0.456						
BW	-0.460	-0.086	-0.125	-0.412					
CC:CO	0.372	-0.824	-0.842	-0.478	0.174				
KO:LD	0.256	-0.463	-0.559	-0.868	0.354	0.562			
KO:SO	0.176	-0.308	-0.374	-0.827	0.614	0.382	0.684		
BW:SO	-0.147	0.272	0.335	0.760	-0.645	-0.352	-0.640	-0.934	
BW:CA	0.156	-0.242	-0.281	-0.419	-0.012	0.257	0.434	0.317	-0.319

Standardized Within-Group Residuals:

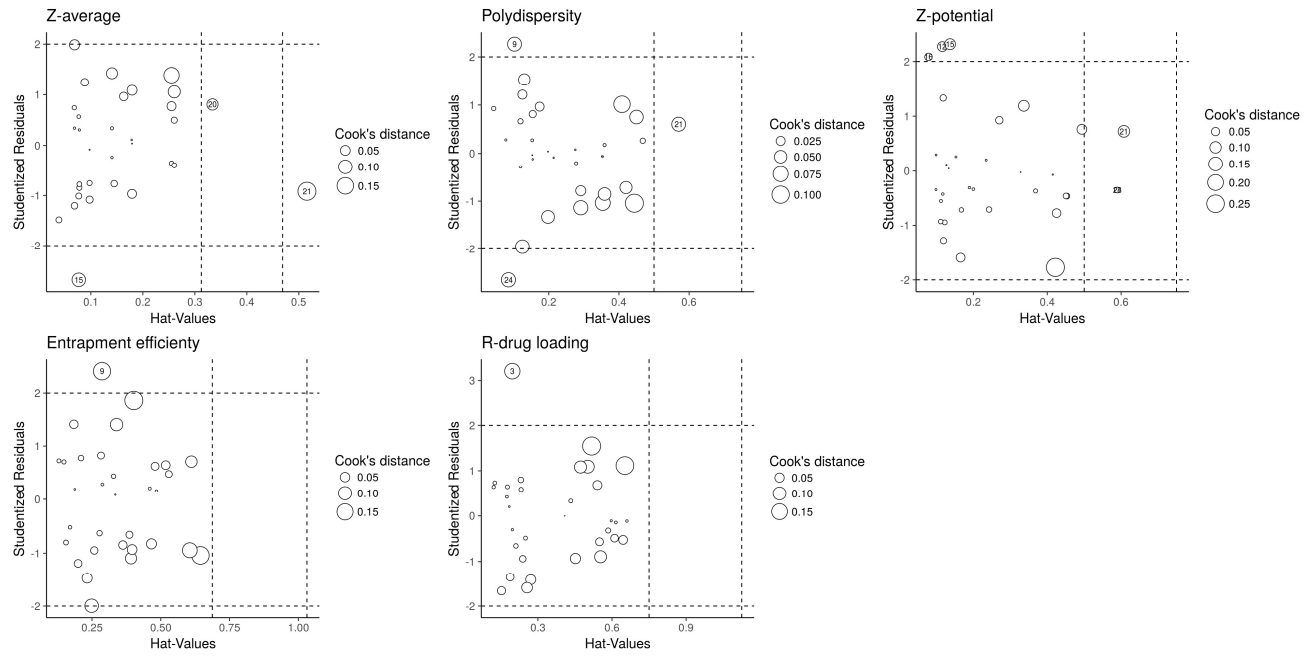
Min	Q1	Med	Q3	Max
-2.0080456	-0.7896294	-0.2065705	0.8728997	2.1036869

Number of Observations: 32

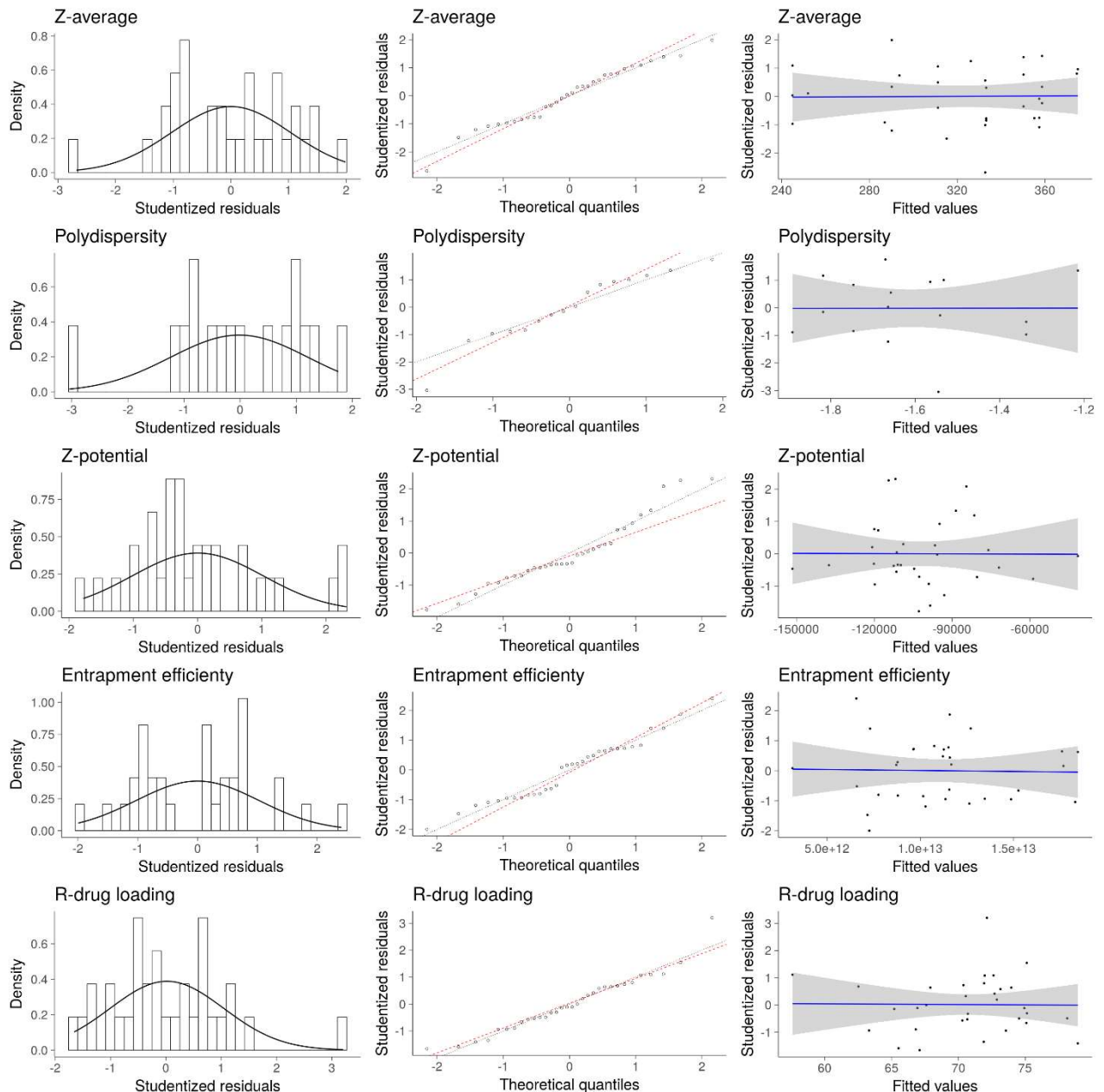
Number of Groups: 2

ANOVA

Model	df	AIC	BIC	logLik	Test	L.Ratio	p-value
IMM	1	3	95.62446	100.02167	-44.81223		
FMM	2	12	73.95932	91.54815	-24.97966	1 vs 2	39.66514 <.0001



SFigure 1. Influence graphs of the models, to the physicochemical outputs: z-average (top left), polydispersity index (top middle), zeta potential (top right), entrapment efficiency (down left) and relative drug loading (down right). Cook's distance measures the model-fitting after deletion of observed values (< 1 is good). Hat-values measures the unusual position of observed values (< 1 is good). It is possible to affirm that none of the samples is configured as outlier.



SFigure 2. Residual analysis of each physicochemical output.

LD drug release:

Free-lidocaine model

Call:

```
lm.default(formula = FL ~ I(19.341 * T^0.556))
```

Residuals:

	Min	1Q	Median	3Q	Max
	-13.4368	-6.5391	0.5132	5.8054	11.4136

Coefficients:

	Estimate	Std. Error	t value	Pr(> t)
(Intercept)	-4.94230	4.21530	-1.172	0.268
I(19.341 * T^0.556)	1.08359	0.08821	12.284	2.34e-07 ***

Signif. codes:	0 ****	0.001 ***	0.01 **	0.05 *' 0.1 '' 1

Residual standard error: 8.471 on 10 degrees of freedom

Multiple R-squared: 0.9378, Adjusted R-squared: 0.9316

F-statistic: 150.9 on 1 and 10 DF, p-value: 2.344e-07

Sample-release model**Call:**

```
lm.default(formula = ES ~ I(10.618 * T^0.517))
```

Residuals:

Min	1Q	Median	3Q	Max
-4.061	-1.365	-0.001	1.831	3.499

Coefficients:

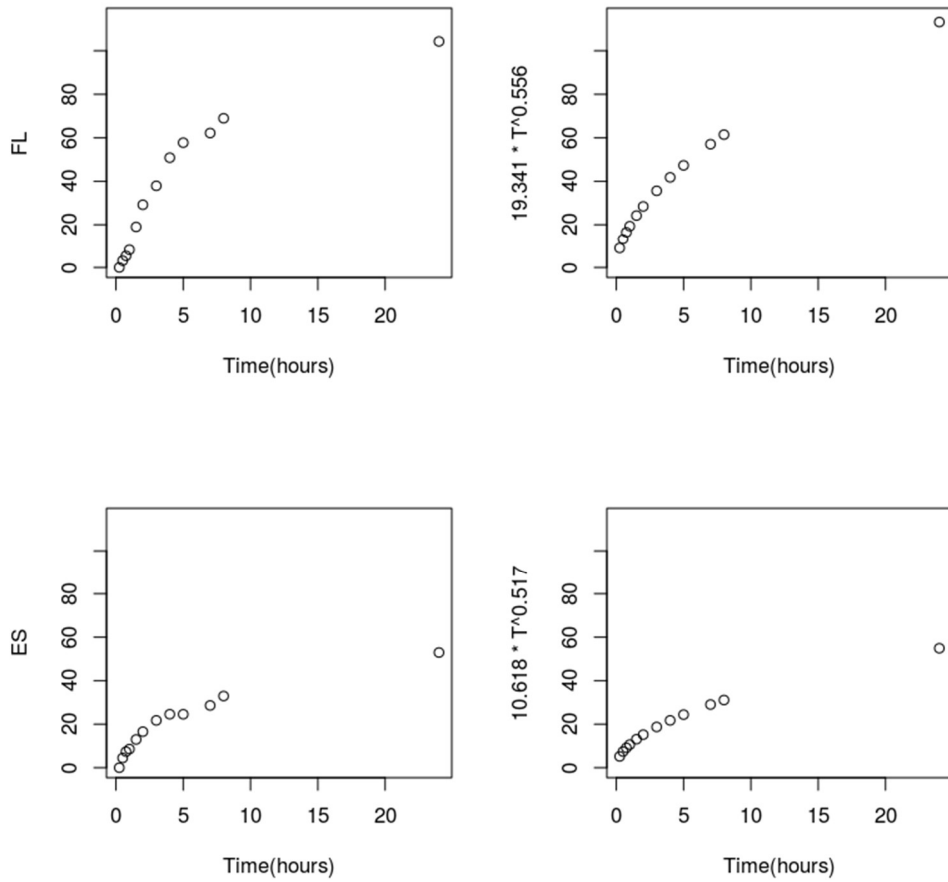
	Estimate	Std. Error	t value	Pr(> t)
(Intercept)	-1.36415	1.30972	-1.042	0.322
I(10.618 * T^0.517)	1.04624	0.05452	19.191	3.21e-09 ***

Signif. codes:	0 ****	0.001 ***	0.01 **	0.05 *' 0.1 '' 1

Residual standard error: 2.499 on 10 degrees of freedom

Multiple R-squared: 0.9736, Adjusted R-squared: 0.9709

F-statistic: 368.3 on 1 and 10 DF, p-value: 3.212e-09



SFigure 3. Free-LD (FL) release profile and the fitted model (top left and right, respectively); Encapsulated-LD (ES) release profile and the fitted model (bottom left and right, respectively).

REFERENCES:

1. Aditya, N. P. *et al.* Development and evaluation of lipid nanocarriers for quercetin delivery: A comparative study of solid lipid nanoparticles (SLN), nanostructured lipid carriers (NLC), and lipid nanoemulsions (LNE). *LWT - Food Sci. Technol.* **59**, 115–121 (2014).
2. Teeranachaideekul, V., Souto, E. B., Junyaprasert, V. B. & Müller, R. H. Cetyl palmitate-based NLC for topical delivery of Coenzyme Q(10) - development, physicochemical characterization and in vitro release studies. *Eur. J. Pharm. Biopharm. Off. J. Arbeitsgemeinschaft Pharm. Verfahrenstechnik EV* **67**, 141–148 (2007).
3. Weber, S., Zimmer, A. & Pardeike, J. Solid Lipid Nanoparticles (SLN) and Nanostructured Lipid Carriers (NLC) for pulmonary application: a review of the state of the art. *Eur. J. Pharm. Biopharm. Off. J. Arbeitsgemeinschaft Pharm. Verfahrenstechnik EV* **86**, 7–22 (2014).
4. Rodrigues da Silva, G. H. *et al.* Optimised NLC: a nanotechnological approach to improve the anaesthetic effect of bupivacaine. *Int. J. Pharm.* **529**, 253–263 (2017).
5. Pathak, K., Keshri, L. & Shah, M. Lipid nanocarriers: influence of lipids on product development and pharmacokinetics. *Crit. Rev. Ther. Drug Carrier Syst.* **28**, 357–393 (2011).
6. Badea, G., Lăcătușu, I., Badea, N., Ott, C. & Meghea, A. Use of various vegetable oils in designing photoprotective nanostructured formulations for UV protection and antioxidant activity. *Ind. Crops Prod. Complete*, 18–24 (2015).
7. Martins, S., Tho, I., Souto, E., Ferreira, D. & Brandl, M. Multivariate design for the evaluation of lipid and surfactant composition effect for optimisation of lipid nanoparticles. *Eur. J. Pharm. Sci. Off. J. Eur. Fed. Pharm. Sci.* **45**, 613–623 (2012).
8. Ribeiro, L. N. M. *et al.* Natural lipids-based NLC containing lidocaine: from pre-formulation to in vivo studies. *Eur. J. Pharm. Sci. Off. J. Eur. Fed. Pharm. Sci.* **106**, 102–112 (2017).

9. Soleimanian, Y., Goli, S. A. H., Varshosaz, J. & Sahafi, S. M. Formulation and characterization of novel nanostructured lipid carriers made from beeswax, propolis wax and pomegranate seed oil. *Food Chem.* **244**, 83–92 (2018).
10. Teeranachaideekul, V., Boonme, P., Souto, E. B., Müller, R. H. & Junyaprasert, V. B. Influence of oil content on physicochemical properties and skin distribution of Nile red-loaded NLC. *J. Control. Release Off. J. Control. Release Soc.* **128**, 134–141 (2008).
11. Wu, C. F. J. & Hamada, M. *Experiments: planning, analysis, and optimization*. (John Wiley & Son Publication, 2009).
12. Bastogne, T. Quality-by-design of nanopharmaceuticals - a state of the art. *Nanomedicine Nanotechnol. Biol. Med.* **13**, 2151–2157 (2017).
13. Li, J., Qiao, Y. & Wu, Z. Nanosystem trends in drug delivery using quality-by-design concept. *J. Control. Release Off. J. Control. Release Soc.* **256**, 9–18 (2017).
14. Müller, R. H., Alexiev, U., Sinambela, P. & Keck, C. M. Nanostructured Lipid Carriers (NLC): The Second Generation of Solid Lipid Nanoparticles. in *Percutaneous Penetration Enhancers Chemical Methods in Penetration Enhancement* (eds. Dragicevic, N. & Maibach, H. I.) 161–185 (Springer Berlin Heidelberg, 2016). doi:10.1007/978-3-662-47862-2_11
15. Doktorovova, S., Shegokar, R. & Souto, E. B. Chapter 30 - Role of Excipients in formulation development and biocompatibility of lipid nanoparticles (SLNs/NLCs). in *Nanostructures for Novel Therapy* (eds. Ficai, D. & Grumezescu, A. M.) 811–843 (Elsevier, 2017). doi:10.1016/B978-0-323-46142-9.00030-X
16. Joshi, M. & Patravale, V. Nanostructured lipid carrier (NLC) based gel of celecoxib. *Int. J. Pharm.* **346**, 124–132 (2008).
17. Lin, Y.-K., Huang, Z.-R., Zhuo, R.-Z. & Fang, J.-Y. Combination of calcipotriol and methotrexate in nanostructured lipid carriers for topical delivery. *Int. J. Nanomedicine* **5**, 117–128 (2010).

18. Schwarz, C., Mehnert, W., Lucks, J. S. & Müller, R. H. Solid lipid nanoparticles (SLN) for controlled drug delivery. I. Production, characterization and sterilization. *J. Controlled Release* **30**, 83–96 (1994).
19. Marcato, P. D. *et al.* Nanostructured polymer and lipid carriers for sunscreen. Biological effects and skin permeation. *J. Nanosci. Nanotechnol.* **11**, 1880–1886 (2011).
20. Ridolfi, D. M. *et al.* Chitosan-solid lipid nanoparticles as carriers for topical delivery of tretinoin. *Colloids Surf. B Biointerfaces* **93**, 36–40 (2012).
21. USP Monographs: Lidocaine. Available at: http://www.pharmacopeia.cn/v29240/usp29nf24s0_m45070.html. (Accessed: 19th May 2016)
22. Ribeiro, L. N. M. *et al.* Nanostructured lipid carriers as robust systems for topical lidocaine-prilocaine release in dentistry. *Eur. J. Pharm. Sci.* **93**, 192–202 (2016).
23. Hall, M. Hadamard matrices of order 16. *Res. Summ.* **1**, 21–26 (1961).
24. Box, G. E. P. & Tyssedal, J. Sixteen Run Designs of High Projectivity for Factor Screening. *Commun. Stat. - Simul. Comput.* **30**, 217–228 (2001).
25. Field, A., Miles, J. & Field, Z. *Discovering statistics using R*. (SAGE Publications, 2012).
26. Box, G. E. P., Hunter, W. G. & Hunter, J. S. *Statistics for Experimenters: Design, Innovation, and Discovery*. (Wiley, 2005).
27. Goldstein, H. *Multilevel statistical models*. (John Wiley & Son Publication, 2011).
28. The United States Pharmacopeial Convention. General Notices and Requirements - Applying to Standards, Tests, Assays, and Other Specifications of the United States Pharmacopeia. (2011). Available at: http://www.usp.org/sites/default/files/usp_pdf/EN/USPNF/USP34-NF29General%20Notices.pdf. (Accessed: 3rd May 2016)

29. Hu, F.-Q. *et al.* Preparation and characterization of stearic acid nanostructured lipid carriers by solvent diffusion method in an aqueous system. *Colloids Surf. B Biointerfaces* **45**, 167–173 (2005).
30. Helgason, T., Awad, T. S., Kristbergsson, K., McClements, D. J. & Weiss, J. Effect of surfactant surface coverage on formation of solid lipid nanoparticles (SLN). *J. Colloid Interface Sci.* **334**, 75–81 (2009).
31. Rose, F. *et al.* Engineering of a novel adjuvant based on lipid-polymer hybrid nanoparticles: A quality-by-design approach. *J. Controlled Release* **210**, 48–57 (2015).
32. Gonzalez-Mira, E., Egea, M. A., Souto, E. B., Calpena, A. C. & Garc?a, M. L. Optimizing flurbiprofen-loaded NLC by central composite factorial design for ocular delivery. *Nanotechnology* **22**, 045101 (2011).
33. Wang, J.-L. *et al.* Preparation and characterization of novel lipid carriers containing microalgae oil for food applications. *J. Food Sci.* **79**, E169-177 (2014).
34. Müller, R. H., Mäder, K. & Gohla, S. Solid lipid nanoparticles (SLN) for controlled drug delivery - a review of the state of the art. *Eur. J. Pharm. Biopharm. Off. J. Arbeitsgemeinschaft Für Pharm. Verfahrenstechnik EV* **50**, 161–177 (2000).
35. Keck, C. M. *et al.* Formulation of solid lipid nanoparticles (SLN): The value of different alkyl polyglucoside surfactants. *Int. J. Pharm.* **474**, 33–41 (2014).
36. Tamjidi, F., Shahedi, M., Varshosaz, J. & Nasirpour, A. Design and characterization of astaxanthin-loaded nanostructured lipid carriers. *Innov. Food Sci. Emerg. Technol.* **26**, 366–374 (2014).
37. Adams, E., Coomans, D., Smeyers-Verbeke, J. & Massart, D. L. Non-linear mixed effects models for the evaluation of dissolution profiles. *Int. J. Pharm.* **240**, 37–53 (2002).
38. Prior, A., Frutos, P. & Correa, C. P. Comparison of Dissolution Profiles: Current Guidelines. in 507–509 (2010).

39. Korsmeyer, R. W., Gurny, R., Doelker, E., Buri, P. & Peppas, N. A. Mechanisms of solute release from porous hydrophilic polymers. *Int. J. Pharm.* **15**, 25–35 (1983).

4. Conclusão

O objetivo geral dessa dissertação foi cumprido com êxito, a saber, desenvolver e caracterizar NLC para encapsular LD, a partir de delineamento não regular de Hall e avaliação das interações excipiente-excipiente via análise multinível.

Especificamente, os estudos de pré-formulação foram importantes para concluir que todos os lipídios naturais selecionados solubilizaram a LD, o que foi importante para o sucesso na eficiência de encapsulação e capacidade de carga das NLC. Ainda, a determinação do coeficiente de partição e alguns estudos preliminares de homogeneidade entre os lipídios corroboraram com os resultados de solubilidade, a saber, LD é mais solúvel em BW e CA (um representante de lipídio sólido e líquido, respectivamente), que apresentam maior homogeneidade e maior coeficiente de partição.

As duas aplicações do delineamento de Hall com análise multinível permitiram avaliar a consistência dos resultados e as tendências em cada caso, que possibilita predizer características físico-químicas de acordo com as quantidades e combinações dos excipientes. As variações nos valores de mínimo e máximo foram importantes para identificar modificações no comportamento dos excipientes, de acordo com suas quantidades. Ademais, o delineamento de Hall permite monitorar de perto as interações entre um grande número de excipientes (até 15), a partir de um número pequeno de formulações (16). Os modelos estatísticos desenvolvidos se mostraram bastante apropriados e elucidaram o comportamento entre os excipientes.

As análises mostraram que CA, CP, CC e PS foram os excipientes que mais interagiram nas diferentes respostas. De modo geral, os excipientes que se destacaram atuaram:

- CP (na melhora das caracterizações físico-químicas);
- BW (melhor homogeneidade com os LL e maior solubilidade da LD em relação ao CP);
- CA (tem efeito no PDI, melhor homogeneidade com BW e maior coeficiente de partição e capacidade de solubilizar LD em relação aos outros LL);

- PS foi o tensoativo que atuou na melhora da %EE;
- CC auxiliou tanto no aumento da %EE quanto na %RCC, o que justifica ser o LL mais utilizado na formulação de NLC.

O perfil de liberação da LD livre e encapsulada em NLC mostrou liberação modificada do fármaco.

Os resultados obtidos fornecem um guia para a formulação de NLC baseado nas análises de interações entre seus excipientes. Isso pode ser comprovado pela NLC formulada com os excipientes que se mostraram atuantes de forma proeminente no sentido de promover uma NLC com menor PDI e altos valores de %EE e %CC. Essa comprovação empírica dos resultados preditos enfatiza o sucesso da metodologia desenvolvida e a possibilidade de sua ampliação no desenvolvimento de outros tipos de nanopartículas.

5. Bibliografia

- ADITYA, N. P. et al. Development and evaluation of lipid nanocarriers for quercetin delivery: A comparative study of solid lipid nanoparticles (SLN), nanostructured lipid carriers (NLC), and lipid nanoemulsions (LNE). **LWT - Food Science and Technology**, v. 59, n. 1, p. 115–121, 1 nov. 2014.
- ARAÚJO, D. R. DE et al. Formulações de anestésicos locais de liberação controlada: aplicações terapêuticas. v. 5, n. 53, p. 663–671, 2003.
- ARAÚJO, D. R. DE; DE PAULA, E.; FRACETO, L. F. Anestésicos locais: Interação com membranas biológicas e com o canal de sódio voltagem dependente. v. 31, n. 7, p. 1775–1783, 2008b.
- ATTAMA, A. A. SLN, NLC, LD: state of the art in drug and active delivery. **Recent Patents on Drug Delivery & Formulation**, v. 5, n. 3, p. 178–187, set. 2011.
- ATTAMA, A. A.; MOMOH, M. A.; BUILDERS, P. F. **Lipid Nanoparticulate Drug Delivery Systems: A Revolution in Dosage Form Design and Development, Recent Advances in Novel Drug Carrier Systems**, PhD. Ali Demir Sezer (Ed.), InTech, DOI: 10.5772/50486. Disponível em: <http://cdn.intechopen.com/pdfs/40253/InTech-Lipid_nanoparticulate_drug_delivery_systems_a_revolution_in_dosage_form_design_and_development.pdf>. Acesso em: 9 maio. 2016.
- BADEA, G. et al. Use of various vegetable oils in designing photoprotective nanostructured formulations for UV protection and antioxidant activity. **Industrial Crops & Products**, v. Complete, n. 67, p. 18–24, 2015.
- BATTAGLIA, L.; GALLARATE, M. Lipid nanoparticles: state of the art, new preparation methods and challenges in drug delivery. **Expert Opinion on Drug Delivery**, v. 9, n. 5, p. 497–508, maio 2012.
- BLUNDELL, E. L. C. J. et al. Characterisation of the protein corona using tunable resistive pulse sensing: determining the change and distribution of a particle's surface charge. **Analytical and Bioanalytical Chemistry**, v. 408, n. 21, p. 5757–5768, 2016.
- BONDI, M. L. et al. Entrapment of an EGFR inhibitor into nanostructured lipid carriers (NLC) improves its antitumor activity against human hepatocarcinoma cells. **Journal of Nanobiotechnology**, v. 12, p. 21, 2014.
- BOX, G. E. P.; HUNTER, W. G.; HUNTER, J. S. **Statistics for Experimenters: Design, Innovation, and Discovery**. second ed. ed. New York: Wiley, 2005.
- BOX, G. E. P.; TYSSEDAL, J. Sixteen Run Designs of High Projectivity for Factor Screening. **Communications in Statistics - Simulation and Computation**, v. 30, n. 2, p. 217–228, 30 abr. 2001.
- BOX, G.; TYSSEDAL, J. Projective Properties of Certain Orthogonal Arrays. **Biometrika**, v. 83, n. 4, p. 950–955, 1996.
- BUTTERWORTH, J. F.; STRICHARTZ, G. R. Molecular mechanisms of local anesthesia: a review. **Anesthesiology**, v. 72, n. 4, p. 711–734, abr. 1990.
- COLLINS, K. D.; WASHABAUGH, M. W. The Hofmeister effect and the behaviour of water at interfaces. **Quarterly Reviews of Biophysics**, v. 18, n. 04, p. 323–422, nov. 1985.

COLLINSWORTH, K. A.; KALMAN, S. M.; HARRISON, D. C. The clinical pharmacology of lidocaine as an antiarrhythmic drug. **Circulation**, v. 50, n. 6, p. 1217–1230, dez. 1974.

DAS, S.; NG, W. K.; TAN, R. B. H. Are nanostructured lipid carriers (NLCs) better than solid lipid nanoparticles (SLNs): development, characterizations and comparative evaluations of clotrimazole-loaded SLNs and NLCs? **European Journal of Pharmaceutical Sciences: Official Journal of the European Federation for Pharmaceutical Sciences**, v. 47, n. 1, p. 139–151, 30 ago. 2012.

DE ARAÚJO, D. R. et al. Strategies for delivering local anesthetics to the skin: focus on liposomes, solid lipid nanoparticles, hydrogels and patches. **Expert Opinion on Drug Delivery**, v. 10, n. 11, p. 1551–1563, 13 ago. 2013.

DE LYRA, M. A. M. et al. Sistemas matriciais hidrofílicos e mucoadesivos para liberação controlada de fármacos. v. 26, n. 5, p. 784–93, 2007.

DE PAULA, E. et al. Drug delivery systems for local anesthetics. **Recent Patents on Drug Delivery & Formulation**, v. 4, n. 1, p. 23–34, jan. 2010.

DE PAULA, E. et al. Micro and nanosystems for delivering local anesthetics. **Expert Opinion on Drug Delivery**, v. 9, n. 12, p. 1505–1524, dez. 2012.

FREITAS, C.; MÜLLERÄ, R. H. Spray-drying of solid lipid nanoparticles (SLN TM). **European Journal of Pharmaceutics and Biopharmaceutics: Official Journal of Arbeitsgemeinschaft Für Pharmazeutische Verfahrenstechnik e.V.**, v. 46, n. 2, p. 145–151, set. 1998.

GANGULY, S.; CHAKRABORTY, S. Sedimentation of nanoparticles in nanoscale colloidal suspensions. **Physics Letters A**, v. 375, n. 24, p. 2394–2399, 13 jun. 2011.

GIBBONS, K. et al. Continuous Lidocaine Infusions to Manage Opioid-Refractory Pain in a Series of Cancer Patients in a Pediatric Hospital. **Pediatric Blood & Cancer**, 19 jan. 2016.

GUSE, C. et al. Biocompatibility and erosion behavior of implants made of triglycerides and blends with cholesterol and phospholipids. **International Journal of Pharmaceutics**, Local Controlled Drug Delivery to the Brain. v. 314, n. 2, p. 153–160, 18 maio 2006.

GUTERRES, S. S.; ALVES, M. P.; POHLMANN, A. R. Polymeric Nanoparticles, Nanospheres and Nanocapsules, for Cutaneous Applications. **Drug Target Insights**, v. 2, p. 147–157, 11 jul. 2007.

HAMADA, M.; WU, C. F. J. Analysis of designed experiments with complex aliasing. **Journal of Quality Technology**, v. 24, p. 130–137, 1 jul. 1992.

HELGASON, T. et al. Effect of surfactant surface coverage on formation of solid lipid nanoparticles (SLN). **Journal of Colloid and Interface Science**, v. 334, n. 1, p. 75–81, 1 jun. 2009.

HERMINGHAUS, A. et al. [Intravenous administration of lidocaine for perioperative analgesia. Review and recommendations for practical usage]. **Der Anaesthesist**, v. 60, n. 2, p. 152–160, fev. 2011.

JENNING, V.; MÄDER, K.; GOHLA, S. H. Solid lipid nanoparticles (SLN) based on binary mixtures of liquid and solid lipids: a (1)H-NMR study. **International Journal of Pharmaceutics**, v. 205, n. 1–2, p. 15–21, 15 set. 2000.

- JIA, L. et al. Nanostructured lipid carriers for parenteral delivery of silybin: Biodistribution and pharmacokinetic studies. **Colloids and Surfaces. B, Biointerfaces**, v. 80, n. 2, p. 213–218, 15 out. 2010.
- JIANG, W. et al. Modeling of nanoparticles' aggregation and sedimentation in nanofluid. **Current Applied Physics**, v. 10, n. 3, p. 934–941, maio 2010.
- JOSHI, M.; PATRAVALE, V. Nanostructured lipid carrier (NLC) based gel of celecoxib. **International Journal of Pharmaceutics**, v. 346, n. 1–2, p. 124–132, 4 jan. 2008.
- KECK, C. M. et al. Formulation of solid lipid nanoparticles (SLN): The value of different alkyl polyglucoside surfactants. **International Journal of Pharmaceutics**, v. 474, n. 1, p. 33–41, 20 out. 2014.
- KINGSLEY, J. D. et al. Nanotechnology: a focus on nanoparticles as a drug delivery system. **Journal of Neuroimmune Pharmacology: The Official Journal of the Society on NeuroImmune Pharmacology**, v. 1, n. 3, p. 340–350, set. 2006.
- KONAN, Y. N.; GURNY, R.; ALLÉMANN, E. Preparation and characterization of sterile and freeze-dried sub-200 nm nanoparticles. **International Journal of Pharmaceutics**, v. 233, n. 1–2, p. 239–252, 21 fev. 2002.
- LACATUSU, I. et al. Highly antioxidant carotene-lipid nanocarriers: synthesis and antibacterial activity. **Journal of Nanoparticle Research**, v. 14, p. 902, 1 jun. 2012.
- LACATUSU, I. et al. Lipid nanoparticles based on omega-3 fatty acids as effective carriers for lutein delivery. Preparation and in vitro characterization studies. **Journal of Functional Foods**, v. 5, n. 3, p. 1260–1269, 1 jul. 2013.
- LAURETTI, G. R. Mechanisms of analgesia of intravenous lidocaine. **Revista Brasileira De Anestesiologia**, v. 58, n. 3, p. 280–286, jun. 2008.
- LEE, J. Drug nano- and microparticles processed into solid dosage forms: Physical properties. **Journal of Pharmaceutical Sciences**, v. 92, n. 10, p. 2057–2068, 1 out. 2003.
- LEE, M. K. et al. Cryoprotectants for freeze drying of drug nano-suspensions: Effect of freezing rate. **Journal of Pharmaceutical Sciences**, v. 98, n. 12, p. 4808–4817, 1 dez. 2009.
- LIU, C.-H.; WU, C.-T. Optimization of nanostructured lipid carriers for lutein delivery. **Colloids and Surfaces A: Physicochemical and Engineering Aspects**, v. 353, n. 2, p. 149–156, 15 jan. 2010.
- LIU, K. et al. Preparation and characterization of 10-hydroxycamptothecin loaded nanostructured lipid carriers. **Drug Development and Industrial Pharmacy**, v. 34, n. 5, p. 465–471, maio 2008.
- MALAMED, S. F. **Manual de Anestesia Local**. 4^a edição ed. Rio de Janeiro: Guanabara Koogan, 2001.
- MARCATO, P. D. et al. Nanostructured polymer and lipid carriers for sunscreen. Biological effects and skin permeation. **Journal of Nanoscience and Nanotechnology**, v. 11, n. 3, p. 1880–1886, mar. 2011.
- MARTINS, S. et al. Multivariate design for the evaluation of lipid and surfactant composition effect for optimisation of lipid nanoparticles. **European Journal of Pharmaceutical Sciences: Official Journal of the European Federation for Pharmaceutical Sciences**, v. 45, n. 5, p. 613–623, 11 abr. 2012.

- MCCARTHY, G. C.; MEGALLA, S. A.; HABIB, A. S. Impact of intravenous lidocaine infusion on postoperative analgesia and recovery from surgery: a systematic review of randomized controlled trials. **Drugs**, v. 70, n. 9, p. 1149–1163, 18 jun. 2010.
- MCLURE, H. A.; RUBIN, A. P. Review of local anaesthetic agents. **Minerva Anestesiologica**, v. 71, n. 3, p. 59–74, mar. 2005.
- MÜLLER, R. H. et al. Cytotoxicity of magnetite-loaded polylactide, polylactide/glycolide particles and solid lipid nanoparticles. **International Journal of Pharmaceutics**, v. 138, n. 1, p. 85–94, 12 jul. 1996.
- MÜLLER, R. H.; SHEGOKAR, R.; KECK, C. M. 20 years of lipid nanoparticles (SLN and NLC): present state of development and industrial applications. **Current Drug Discovery Technologies**, v. 8, n. 3, p. 207–227, set. 2011.
- PARDEIKE, J.; HOMMOSS, A.; MÜLLER, R. H. Lipid nanoparticles (SLN, NLC) in cosmetic and pharmaceutical dermal products. **International Journal of Pharmaceutics**, v. 366, n. 1–2, p. 170–184, 21 jan. 2009.
- PARDESHI, C. et al. Solid lipid based nanocarriers: an overview. **Acta Pharmaceutica (Zagreb, Croatia)**, v. 62, n. 4, p. 433–472, dez. 2012.
- PATHAK, K.; KESHRI, L.; SHAH, M. Lipid nanocarriers: influence of lipids on product development and pharmacokinetics. **Critical Reviews in Therapeutic Drug Carrier Systems**, v. 28, n. 4, p. 357–393, 2011.
- PUBCHEM. **lidocaine** | **C14H22N2O** - PubChem. Disponível em: <<https://pubchem.ncbi.nlm.nih.gov/compound/lidocaine>>. Acesso em: 2 maio. 2016.
- PUGLIA, C.; BONINA, F. Lipid nanoparticles as novel delivery systems for cosmetics and dermal pharmaceuticals. **Expert Opinion on Drug Delivery**, v. 9, n. 4, p. 429–441, abr. 2012.
- QUEIRÓZ, V. A. **Avaliação das atividades citotóxica, anestésica e da farmacocinética da Bupivacaína complexada com Hidroxipropil-beta-ciclodextrina, em associação com Sufentanil**. Dissertação de Mestrado em Biologia Funcional e Molecular—Campinas: Universidade Estadual de Campinas, 2012.
- RAHMAN, H. S. et al. Zerumbone-loaded nanostructured lipid carriers: preparation, characterization, and antileukemic effect. **International Journal of Nanomedicine**, v. 8, p. 2769–2781, 2013.
- RIBEIRO, L. N. M. et al. Nanostructured lipid carriers as robust systems for topical lidocaine-prilocaine release in dentistry. **European Journal of Pharmaceutical Sciences**, v. 93, p. 192–202, 10 out. 2016.
- RIBEIRO, L. N. M. et al. Natural lipids-based NLC containing lidocaine: from pre-formulation to in vivo studies. **European Journal of Pharmaceutical Sciences: Official Journal of the European Federation for Pharmaceutical Sciences**, v. 106, p. 102–112, 30 ago. 2017.
- RIDOLFI, D. M. et al. Chitosan-solid lipid nanoparticles as carriers for topical delivery of tretinoin. **Colloids and Surfaces. B, Biointerfaces**, v. 93, p. 36–40, 1 maio 2012.
- RODRIGUES DA SILVA, G. H. et al. Optimised NLC: a nanotechnological approach to improve the anaesthetic effect of bupivacaine. **International Journal of Pharmaceutics**, v. 529, n. 1, p. 253–263, 30 ago. 2017.

SAUPE, A. et al. Solid lipid nanoparticles (SLN) and nanostructured lipid carriers (NLC) -- structural investigations on two different carrier systems. **Bio-Medical Materials and Engineering**, v. 15, n. 5, p. 393–402, 2005.

SCHWARZ, C. et al. Solid lipid nanoparticles (SLN) for controlled drug delivery. I. Production, characterization and sterilization. **Journal of Controlled Release**, v. 30, n. 1, p. 83–96, 1 abr. 1994.

SCHWARZ, C.; MEHNERT, W. Solid lipid nanoparticles (SLN) for controlled drug delivery. II. Drug incorporation and physicochemical characterization. **Journal of Microencapsulation**, v. 16, n. 2, p. 205–213, abr. 1999.

SOLEIMANIAN, Y. et al. Formulation and characterization of novel nanostructured lipid carriers made from beeswax, propolis wax and pomegranate seed oil. **Food Chemistry**, v. 244, p. 83–92, 1 abr. 2018.

SOUTO, E. B.; ALMEIDA, A. J.; MÜLLER, R. H. Lipid Nanoparticles (SLN®, NLC®) for Cutaneous Drug Delivery:Structure, Protection and Skin Effects. **Journal of Biomedical Nanotechnology**, v. 3, n. 4, p. 317–331, 1 dez. 2007.

STARK, B.; PABST, G.; PRASSL, R. Long-term stability of sterically stabilized liposomes by freezing and freeze-drying: Effects of cryoprotectants on structure. **European Journal of Pharmaceutical Sciences: Official Journal of the European Federation for Pharmaceutical Sciences**, v. 41, n. 3–4, p. 546–555, 20 nov. 2010.

STRICHARTZ, G. R. Novel ideas of local anaesthetic actions on various ion channels to ameliorate postoperative pain. **British Journal of Anaesthesia**, v. 101, n. 1, p. 45–47, jul. 2008.

STRICHARTZ, G. R.; RITCHIE, J. M. **Local Anesthetics, Handbook of Experimental Pharmacology**. Berlim: Springer Verlag, 1987.

TEERANACHAIDEEKUL, V. et al. Cetyl palmitate-based NLC for topical delivery of Coenzyme Q(10) - development, physicochemical characterization and in vitro release studies. **European Journal of Pharmaceutics and Biopharmaceutics: Official Journal of Arbeitsgemeinschaft Fur Pharmazeutische Verfahrenstechnik e.V**, v. 67, n. 1, p. 141–148, ago. 2007.

TEERANACHAIDEEKUL, V. et al. Influence of oil content on physicochemical properties and skin distribution of Nile red-loaded NLC. **Journal of Controlled Release: Official Journal of the Controlled Release Society**, v. 128, n. 2, p. 134–141, 4 jun. 2008.

USP Monographs: **Lidocaine.** Disponível em: <http://www.pharmacopeia.cn/v29240/usp29nf24s0_m45070.html>. Acesso em: 19 maio. 2016.

VAN TUIJL, I. et al. The effect of addition of intrathecal clonidine to hyperbaric bupivacaine on postoperative pain and morphine requirements after Caesarean section: a randomized controlled trial. **British Journal of Anaesthesia**, v. 97, n. 3, p. 365–370, set. 2006.

VARSHOSAZ, J.; ESKANDARI, S.; TABBAKHIAN, M. Freeze-drying of nanostructure lipid carriers by different carbohydrate polymers used as cryoprotectants. **Carbohydrate Polymers**, v. 88, n. 4, p. 1157–1163, 16 maio 2012.

WEBER, S.; ZIMMER, A.; PARDEIKE, J. Solid Lipid Nanoparticles (SLN) and Nanostructured Lipid Carriers (NLC) for pulmonary application: a review of the state of the art. **European Journal of**

Pharmaceutics and Biopharmaceutics: Official Journal of Arbeitsgemeinschaft Für Pharmazeutische Verfahrenstechnik e.V., v. 86, n. 1, p. 7–22, jan. 2014.

WISSING, S. A.; KAYSER, O.; MÜLLER, R. H. Solid lipid nanoparticles for parenteral drug delivery. **Advanced Drug Delivery Reviews**, v. 56, n. 9, p. 1257–1272, 7 maio 2004.

WU, L.; ZHANG, J.; WATANABE, W. Physical and chemical stability of drug nanoparticles. **Advanced Drug Delivery Reviews**, Nanodrug Particles and Nanoformulations for Drug Delivery. v. 63, n. 6, p. 456–469, 30 maio 2011.

ZUR MÜHLEN, A.; SCHWARZ, C.; MEHNERT, W. Solid lipid nanoparticles (SLN) for controlled drug delivery--drug release and release mechanism. **European Journal of Pharmaceutics and Biopharmaceutics: Official Journal of Arbeitsgemeinschaft Für Pharmazeutische Verfahrenstechnik e.V.**, v. 45, n. 2, p. 149–155, mar. 1998.

6. Anexos

6.1. Artigos submetidos para publicação

Current protein drugs: biological function, administration route, dosage form and excipient profiling

Autores: Geraldes, D. C., Beraldo-de-Araújo, V. L., Oliveira-Nascimento, L.

Revista: European Journal of Pharmaceutical Sciences

6.2. Anais de Congresso



I International Symposium on
Drug Delivery Systems

ANTIMICROBIAL ACTIVITY OF DIBUCAINA ENCAPSULATED IN NANOSTRUCTURED LIPID CARRIER

Beraldo de Araujo, V. L.¹, de Paula, E.¹, Lancellotti, M.¹, Oliveira-Nascimento, L.¹

¹Department of Biochemistry and Tissue Biology - University of Campinas - Campinas - Brazil

E-mail: vivi.beraldo@gmail.com

Keywords: Nanoparticles – NLC – Dibucaine – MIC

1. Introduction

Nanocarriers are able to modify solubility, toxicity and dissolution of carried drugs. The lipid nanocarriers outstand from polymeric ones due to their biocompatibility, reproducibility and loading efficiency of hydrophobic drugs¹. Nanostructured Lipid Carriers (NLCs) are a recent generation of this class. NLC is made of a solid lipid and at least one liquid lipid at room temperature². Dibucaine (DBC) is a hydrophobic local anesthetic applied topically due to its high toxicity. In an attempt to avoid the side effects and prolong the beneficial effects, DBC has been encapsulated into NLC. This work aimed to verify the antimicrobial properties of both pure and encapsulated DBC, in addition to their already tested anesthetic effects.

2. Methods

NLC production: NLC was produced by hot homogenization method³. Oily phase was heated and DBC was solubilized into this phase. Then, aqueous phase was dripped to oily phase under high speed agitation (10,000 rpm) using a Turrax blender (IKA WerkeStaufen, Germany) by 3 min, followed by sonication with titanium micro-tip (potency 50W, 20kHz), in cycles of 30s by 30 min. The nanoemulsion was cooled on ice bath until 25°C and stored at 4°C.

NLC characterization: Average particle size (z-average), polydispersity index (PDI) and zeta potential (ZP) of the NLC samples were measured in Zetasizer Nano ZS90 (Malvern Instruments, UK).

Antimicrobial tests: MIC determination was performed by the microdilution method (as described by CLSI) with *Pseudomonas aeruginosa* ATCC 27853, *Escherichia coli* ATCC 25922 and *Staphylococcus aureus* ATCC 25923. The agar diffusion test was checked with *E. coli* ATCC 25922 and *S. aureus* ATCC 25923 on Müller-Hinton Agar plates.

3. Results

The NLC and NLC-DBC presented, respectively, z-average size of 239.6 nm and 193.3 nm; PDI of 0.221 and 0.239; ZP of -23.8 mV and -1.37 mV. The colloidal stability was maintained for at least two weeks. Pure DBC presented MIC of 125 µg/mL for *E. coli*, 500 µg/mL for *S. aureus* and 500 µg/mL for *P. aeruginosa*. NLC-DBC presented undetectable MIC for all bacteria because of excessive turbidity. The agar diffusion test shown that DBC and NLC-DBC presented similar inhibition zones for *E. coli* and *S. aureus*.

4. Conclusion

NLC and NLC-DBC have shown good stability and an adequate z-average and PDI results. ZP of NLC-DBC is lower in module than ZP of NLC, possibly due to nanoparticle structural changes upon addition of DBC. MIC results have shown antimicrobial activity of pure DBC, especially for *E. coli*, and the agar diffusion test confirms that the encapsulated drug maintains its antimicrobial activity. The presented data indicates that DBC and NLC-DBC can be considered as an adjunct to traditional antimicrobial clinical therapy.

Acknowledgments

FAPESP (2014/14457-5) and CAPES for financial support.

References

1. Müller, R. H., Shegokar, R. & Keck, C. M. *Curr. Drug Discov. Technol.* **8**, 207–227 (2011).
2. Pardeike, J., Hommoss, A. & Müller, R. H.. *Int. J. Pharm.* **366**, 170–184 (2009).
3. Barbosa, R. M. et al. Cytotoxicity of solid lipid nanoparticles and nanostructured lipid carriers containing the local anesthetic dibucaine designed for topical application. *J. Phys. Conf. Ser.* **429**, 012035 (2013).

DEVELOPMENT OF LIDOCAINE-LOADED NANOSTRUCTURED LIPID CARRIER TO INTRAVENOUS SUSTAINED RELEASE

BERALDO DE ARAÚJO, V. L.¹; PELEGRINE, A.C.M.²; DE PAULA, E.¹;
OLIVEIRA-NASCIMENTO, L.^{1,2}

¹Department of Biochemistry and Tissue Biology, Biology Institute, University of Campinas, Campinas, São Paulo, Brazil

²Faculty of Pharmaceutical Sciences, University of Campinas, Campinas, São Paulo, Brazil

INTRODUCTION: Nanostructured Lipid Carriers (NLC) are a recent generation of lipid nanocarriers, made of a solid lipid and at least one oil. They are biocompatible, reproducible and have an efficient capacity to load hydrophobic drugs. Lidocaine (LDC) is a hydrophobic local anesthetic broadly used for over 50 years. LDC intravenous administration is made by infusion or multiple bolus because of its short plasmatic half-life, which can be avoided by applying a drug delivery system to maintain LDC in an effective plasmatic concentration for a long period, also reducing its toxicity. In an attempt to prolong the beneficial effects and avoid the side effects, LDC has been encapsulated into NLC.

OBJECTIVES: To develop and characterize lidocaine-loaded NLC to intravenous sustained release.

METHODS: *Screening of lipids:* the lipids were selected according to their origin, melting temperatures, drug solubility and parenteral applicability. **NLC production:** NLC was produced using selected vegetable lipids and super refined oils by hot homogenization method. **NLC characterization:** Average particle size (z-average), polydispersity index (PDI) and zeta potential (ZP) of the NLC samples were measured. **Thermal profile:** Crystallization and melting profile of the excipients were obtained by Differential scanning calorimetry (DSC).

RESULTS: Cetyl palmitate and beeswax were selected as solid lipids; mygliol, castor, sesame, cotton seeds and corn oils were selected as liquid lipids. Z-average were between 200-300nm, PDI between 0,16 and 0,28 and ZP between -55- -12mV. Crystallization and melting profile were according to the range determined by USP.

CONCLUSION: All the formulations presented a good z-average and PDI to a parenteral application, and the negative values of ZP indicate certain formulation stability. DSC analysis show the purity of excipients and the presence of them in the NLC thermal profiles.

KEYWORDS: NLC – LIDOCAINE – LIPIDS

6.3. Declaração – Bioética e Biossegurança



COORDENADORIA DE PÓS-GRADUAÇÃO
INSTITUTO DE BIOLOGIA
Universidade Estadual de Campinas
Caixa Postal 6109. 13083-970, Campinas, SP, Brasil
Fone (19) 3521-6378. email: cpgib@unicamp.br



DECLARAÇÃO

Em observância ao §5º do Artigo 1º da Informação CCPG-UNICAMP/001/15, referente a Bioética e Biossegurança, declaro que o conteúdo de minha Dissertação de Mestrado, intitulada "**CARREADORES LIPÍDICOS NANOESTRUTURADOS (NLC) COM LIDOCAÍNA: SCREENING POR DELINEAMENTO DE HALL**", desenvolvida no Programa de Pós-Graduação em Biociências e Tecnologia de Produtos Bioativos do Instituto de Biologia da Unicamp, não versa sobre pesquisa envolvendo seres humanos, animais ou temas afetos a Biossegurança.

Assinatura: _____
Nome do(a) aluno(a): Viviane Lucia Beraldo de Araújo

Assinatura: _____
Nome do(a) orientador(a): Profa. Dra. Laura de Oliveira Nascimento

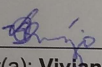
Data: Campinas, 6 de abril de 2018.

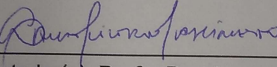
6.4. Declaração – Direitos autorais

Declaração

As cópias de artigos de minha autoria ou de minha co-autoria, já publicados ou submetidos para publicação em revistas científicas ou anais de congressos sujeitos a arbitragem, que constam da minha Dissertação/Tese de Mestrado/Doutorado, intitulada **CARREADORES LIPÍDICOS NANOESTRUTURADOS (NLC) COM LIDOCAÍNA: SCREENING POR DELINEAMENTO DE HALL**, não infringem os dispositivos da Lei n.º 9.610/98, nem o direito autoral de qualquer editora.

Campinas, 06 de abril de 2018.

Assinatura : 
Nome do(a) autor(a): **Viviane Lucia Beraldo de Araújo**
RG n.º 35.987.080-6

Assinatura : 
Nome do(a) orientador(a): **Profa. Dra. Laura de Oliveira Nascimento**
RG n.º 29.992.007-0